Morphological change of vesicle and cell membranes by interaction with domain-swapped cytochrome *c* oligomers

---

ドメインスワップシトクロム *c* 多量体との相互作用による ベシクルおよび細胞膜の形態変化

ACADEMIC DISSERTATION

SENDY JUNEDI

2014 March

Graduate School of Materials Science

Nara Institute of Science and Technology

Supramolecular Science

Contents

List of Abbreviation

ATP	:	Adenosine triphosphate
CL	:	Cardiolipin
TCA	:	Tricarboxylic acid
NADH	:	Reduced nicotinamide adenine dinucleotide
$FADH_2$	:	Reduced flavin adenine dinucleotide
IMM	:	Inner mitochondrial membrane
Cyt *c*	:	Cytochrome *c*
ADP	:	Adenosine diphosphate
AIF	:	Apoptosis-inducing factor
Smac/DIABLO	:	Second mitochondria-derived activator of caspase/direct inhibitor of apoptosis-binding protein with low pI
HtrA2	:	High temperature requirement A2
Cys	:	Cysteine
Lys	:	Lysine
His	:	Histidine
Met	:	Methionine

pI	:	Isoelectric point
SDS	:	Sodium dodecyl sulfate
Apaf-1	:	Apoptotic protease activating factor 1
dATP	:	Deoxyadenosine triphosphate
DNA		Deoxyribonucleic acid
OMM	:	Outer mitochondrial membrane
Bcl-2	:	B-cell lymphoma 2
BAX	:	Bcl-2-associated X
BAK	:	Bcl-2 homologous antagonist/killer
PC	:	Phosphatidylcholine
PG	:	Phosphatidylglycerol
PE	:	Phosphatidylethanolamine
PS	:	Phosphatidylserine
TOCL	:	Tetraoleoyl cardiolipin
DOPA	:	Dioleoyl phosphatidic acid
$DOPIP_3$	:	Dioleoyl phosphatidylinositol triphosphate
$DOPIP_2$	:	Dioleoyl phosphatidylinositol diphosphate
DOPS	:	Dioleoyl phosphatidylserine

SUVs	:	Small unilamellar vesicles
LUVs	:	Large unilamellar vesicles
DOPG	:	Dioleoyl phosphatidylglycerol
DPPG	:	1,2-dipalmitoyl-*sn*-glycero-3-phosphoglycerol
DMPC	:	1,2-dimyristoyl-*sn*-glycero-3-phosphocholine
DSC	:	Differential scanning calorimetry
T_m	:	Phase transition temperature
GUVs	:	Giant unilamellar vesicles
N-Rh-PE	:	*N*-(lissamine rhodamine B)-1,2-dihexadecanoyl-*sn*-glycero-3-phosphoethanolamine, triethylammonium salt
ITO	:	Indium tin oxide
FPLC	:	Fast protein liquid chromatography
PBS	:	Phosphate-buffered saline
DMEM	:	Dulbecco's modified Eagle's medium
FBS	:	Fetal bovine serum
NP-40	:	Nonyl phenoxypolyethoxylethanol
SDS-PAGE	:	Sodium dodecyl sulfate-polyacrylamide gel electrophoresis
TMBZ	:	3,3',5,5'-tetramethylbenzidine

Chapter 1

General introduction

1-1 Cell and mitochondrion

The fundamental unit of life is cell (*1*). The cell (Figure 1.1) is a membrane-enclosed unit, which is filled with a concentrated aqueous solution containing various substances. It endows the ability to grow and reproduce itself. Inside the cell, there are components enclosed by membranes, namely organelles which perform specialized functions in the cell. The external membrane of the cell (about 5 nm thick) is called “plasma membrane”, whereas a similar membrane surrounding the organelles is called “internal membrane”. For the cell activities, the eukaryotic cell needs a basic chemical fuel, adenosine triphosphate (ATP), which is generated in an essential organelle, mitochondrion.

Mitochondrion consists of an outer and inner membrane system (*2*, *3*). The membranes divide the organelle into two compartments; one in the center of the mitochondrion called the matrix, and the other between the outer and inner membranes called the intermembrane space (Figure 1.1). The outer membrane of the mitochondrion contains of lipids by approximately 50 percent in weight (*3*). The outer membrane also contains many porin proteins, which form large aqueous channels through the lipid bilayer. Because of the porin protein, the outer membrane is permeable, allowing molecules up to about 10,000 Da to pass freely the outer membrane to the

intermembrane space. In contrast, the ratio of protein to lipid in the inner membrane is more than 3:1 in weight (*3*). The inner membrane is devoid of cholesterol and rich in cardiolipin (CL) (Figure 1.2), which is a phospholipid possessing two negatively charged phosphate groups and four hydrophobic acyl chains. As illustrated in Figure 1.1, the inner membrane forms a series of infoldings, known as cristae which greatly increase the amount of surface available for ATP production (*2*). In contrast to the outer membrane, the inner membrane is highly impermeable. However, the inner membrane contains a variety of transport proteins that make small molecules required in the matrix permeable to the membrane.

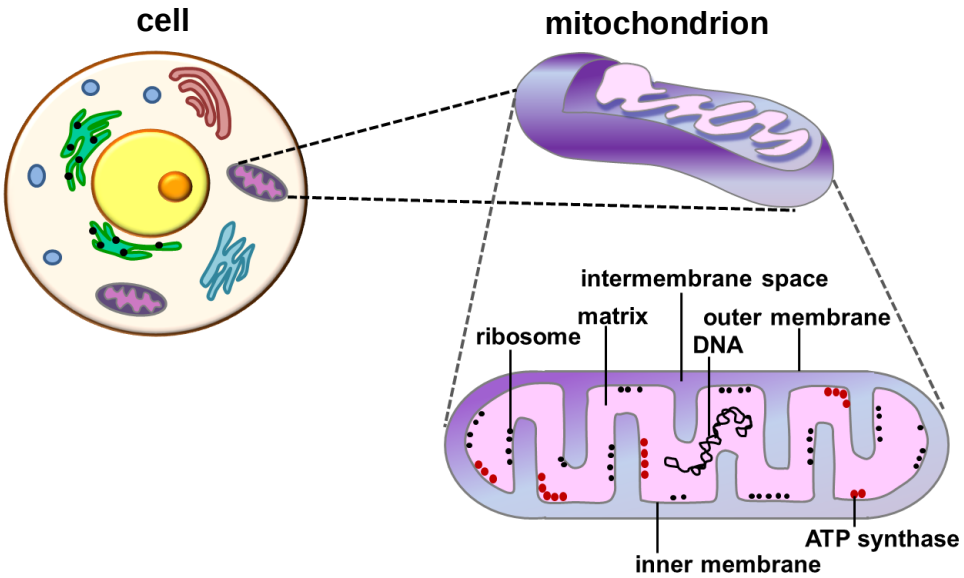

Figure 1.1. Schematic diagram of cell and mitochondrion structure (*3*).

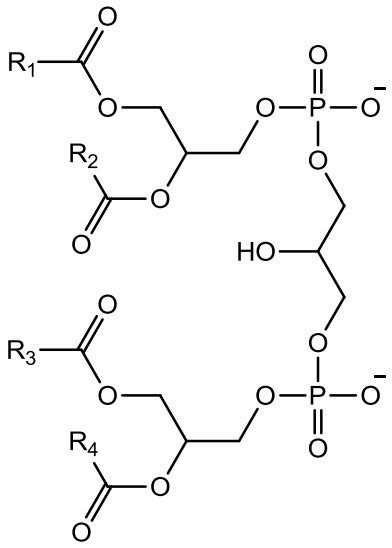

Figure 1.2. Chemical structure of CL. R_1, R_2, R_3, and R_4 are alkyl groups.

Products of the catabolic pathway of polysaccharides, fats, and proteins in the cytosol are fed into the citric acid or tricarboxylic acid (TCA) cycle in the mitochondrial matrix (*2*, *3*). The TCA cycle deposits electrons to the reduced coenzymes (NADH and $FADH_2$), which transfer electrons through the respiratory chain (electron-transport chain) in the inner mitochondrial membrane (IMM). The respiratory chain is composed of membrane-bound electron carriers: Complex I (NADH dehydrogenase), Complex II (succinate dehydrogenase), Complex III (cytochrome bc_1 complex), Complex IV (cytochrome *c* oxidase), ubiquinone, and cytochrome *c* (cyt *c*). The energy released by the respiratory chain is utilized to pump protons across the IMM from the matrix to the intermembrane space, producing an electrical pH potential across the inner membrane

(*1*, *4*). The protein complex, ATP synthase, makes use of the membrane potential to accomplish phosphorylation of adenosine diphosphate (ADP) to ATP (Figure 1.3).

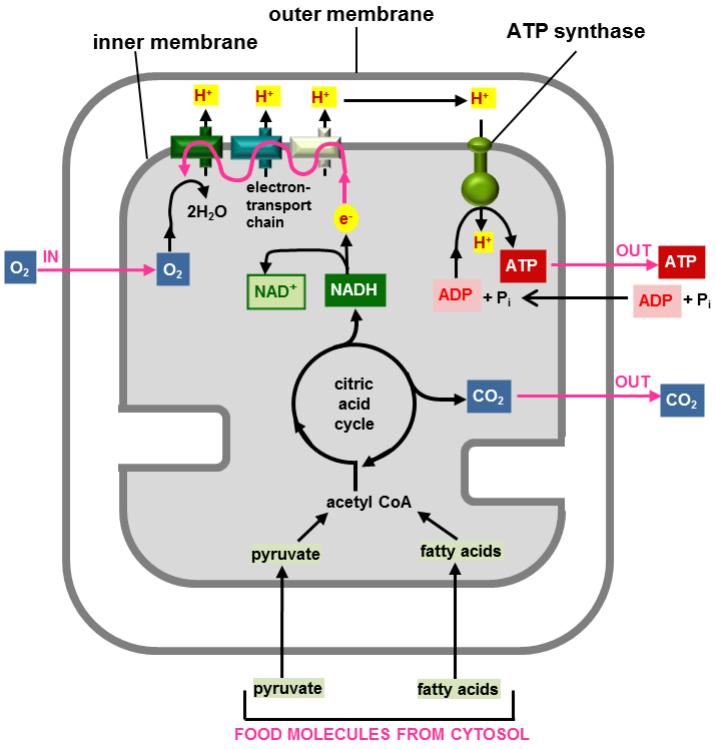

Figure 1.3. Schematic diagram of energy-generating metabolism in mitochondrion (*2*).

In addition to the supply of cellular energy, the mitochondrion is involved in other tasks such as signaling, cellular differentiation, programmed cell death (apoptosis), as well as the control of the cell cycle and cell growth (*5*). Dysregulation of apoptosis contributes to half of all human diseases, and the role of the mitochondron in apoptosis has been paid attention recently. The mitochondrial apoptotic pathway involves the

release of pro-apoptotic proteins including the apoptosis-inducing factor (AIF), Smac/DIABLO, HtrA2/Omi, and cyt *c*, from the mitochondron to the cytosol (*6*). Subsequently, the pro-apoptotic proteins activate the caspase cascade in the cytosol, leading to cell death.

1-2 Structure and function of cytochrome *c*

Cyt *c* is a protein bound to the mitochondria in almost all living organisms (animals, plants, and many unicellular organisms). It has important roles in both respiratory chain and apoptosis in mitochondrion. Cyt *c* (Figure 1.4A) is a single-chain hemoprotein composed of 104 amino acids with molecular weight of 12,400 Da (*7*, *8*). The heme cofactor, as a prosthetic group, in cyt *c* lies within a structural crevice, and is covalently attached to the polypeptide chain by two thioether bridges formed with Cys14 and Cys17 (Figure 1.4B). The four coordination positions of the heme iron are occupied by the four pyrrole nitrogen atoms of a porphyrin ring. The fifth and sixth coordination positions located on the axial side of the heme are occupied by an imidazole nitrogen atom of histidine18 (His18) and a sulfur atom of methionine80 (Met80). Cyt *c* is composed of three major (N-terminus, C-terminus, and 60-s helices)

helical elements interconnected by the strands of the polypeptide chain, and fold into a roughly globular shape (*8*).

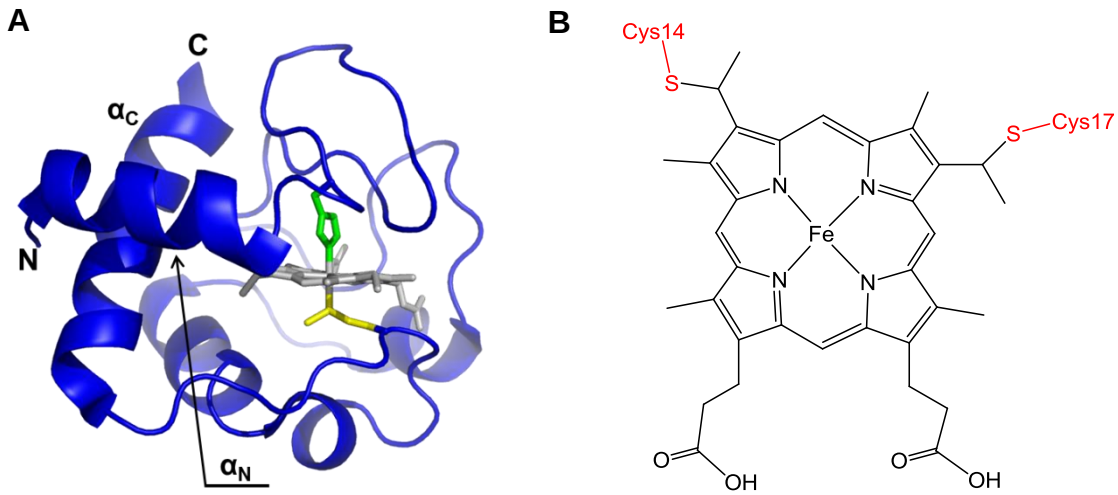

Figure 1.4. (A) Structure of horse cyt *c* (PDB ID code:1HRC). The heme cofactor is shown as a gray stick model. Side-chain atoms of His18 and Met80 are shown as green and yellow stick models, respectively. The N and C termini and the N- and C-terminal helices are labeled as N, C, α_N, and α_C, respectively. (B) Molecular structure of heme *c*. Cys14 and Cys17, which form thioether bridges with the heme cofactor, are shown in red color.

One of the most striking features of cyt *c* is its high content of lysines (19 residues in horse cyt *c*) on the surface *(7)*. Cyt *c* from horse heart (denoted as horse cyt *c*) also carries two arginine residues, but only 12 acidic residues (aspartic acid and glutamic acid) on its surface. Therefore, cyt *c* is a basic protein, with an isoelectric point (pI) near pH 10 for human and horse cyt *c* (*9*). At neutral pH, the net charge of amino acids residues of horse cyt *c* is +9 (*10*). The formal net charge of the heme cofactor of

cyt *c* is +1 for the oxidized protein, and 0 for the reduced protein (*11*). In addition to the positively charged residues on the surface, cyt *c* also possesses hydrophobic residues, where the side chains of most of the hydrophobic residues point inward toward the heme, to form a hydrophobic interior *(7)*.

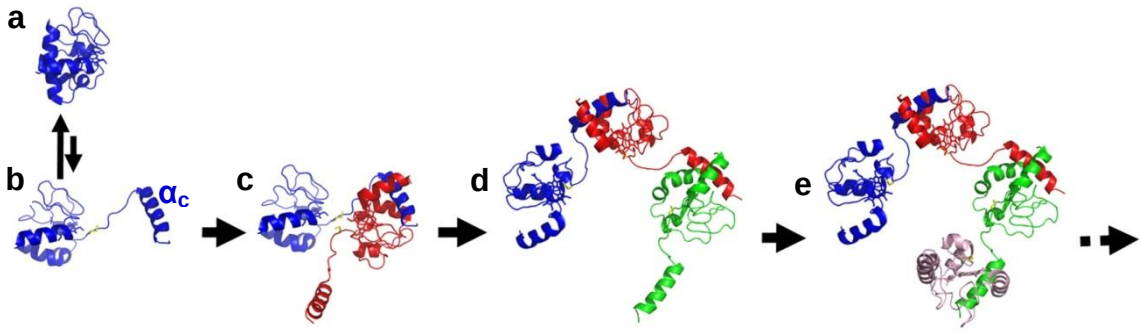

Figure 1.5. Scheme of cyt *c* oligomerization by domain-swapping mechanism. Crystal structure of monomeric cyt *c* (a) (PDB ID code:1HRC). Model of monomeric (b), dimeric (c), trimeric (d), and tetrameric (e) cyt *c* in solution (*12*).

Horse cyt *c* has been reported to form oligomers by successive domain swapping at the C-terminal helix (Figure 1.5) (*12*). By perturbation with an addition of ethanol or sodium dodecyl sulfate (SDS), cyt *c* may convert to a C-terminal open-ended form, and the corresponding C-terminal region of another cyt *c* molecule may occupy the vacant area, producing oligomers. In domain-swapped oligomeric cyt *c*, Met80 is dissociated from the heme iron and the hydrophobic interior of cyt *c* becomes more accessible to the solvent compared to the monomer. Domain-swapped oligomeric cyt *c* maintains the

secondary structures of the monomer, whereas its surface possesses a larger area and more charges compared to the monomer. At present, the existence of domain swapping of cyt *c in vivo* has not been known, and its biological function is as yet unrevealed.

In cell, cyt *c* normally functions by attaching to the outer surface of the IMM, mainly by association with CL (*13*). The membrane-bound cyt *c* is suggested to participate as a single electron carrier from Complex III to Complex IV in the final step of the respiratory chain (*14*). The heme iron atom of cyt *c* alternates between the +2 and +3 oxidation state when the molecule interacts with Complex III or Complex IV (*7*). The solvent-exposed heme edge surrounded by lysines residues, is considered to be a relevant surface site for electron transfer, supported by electrostatic interaction between cyt *c* and redox partner proteins (*7, 15*). In mammalians cells, the electron transfer carried out by cyt *c*, is the proposed rate-limiting step of the respiratory chain under physiological conditions (*14*), and is tightly regulated by the ATP/ADP ratio (*16*) and tyrosine phosphorylation of cyt *c (17, 18)*.

In 1996, Liu *et al.* found that the release of cyt *c* from the mitochondrion to the cytosol can induce apoptosis, and the addition of exogenous cyt *c* to the cytosol causes a similar response (*19*). Cyt *c* and cytosolic apoptotic protease activating factor 1 (Apaf-1), along with deoxyadenosine triphosphate (dATP), interact in the cytosol to

form apoptosome, a complex which activates caspase-9, allowing subsequent activation of the executioners caspases, caspase-3 and caspase-7 (Figure 1.6) (*6*). Normally, effector caspases are responsible for the cleavage of various proteins and lead to apoptosis (*20*).

In the presence of apoptotic stimulus, such as DNA damage and metabolic stress, cyt *c* in the mitochondrion is released to the cytosol through a two-step process, consisting of the detachment of this protein from IMM, followed by permeabilization of the outer mitochondrial membrane (OMM) (*13*). One of the proposed mechanisms to release CL-associated cyt *c* is through the oxidation of CL by a cyt *c*-CL complex and a reactive oxygen species (Figure 1.6) (*21, 22*). Calcium ion, which is released from the endoplasmic reticulum and translocated to IMM, can also induce the detachment of cyt *c* from CL by weakening the electrostatic interaction between cyt *c* and CL (*23*). Mobilized cyt *c* in the intermembrane space is suggested to translocate through OMM to the cytosol by the opening of a permeability transition pore, which is assembled at the contact sites of IMM and OMM (*24*), or by pore formation induced by oligomerization of Bcl-2-homology proteins, BAX, and BAK, in OMM (*25*). Although many mechanisms have been suggested, the exact mechanism by which cyt *c* is released from the mitochondria during apoptosis remains unclear.

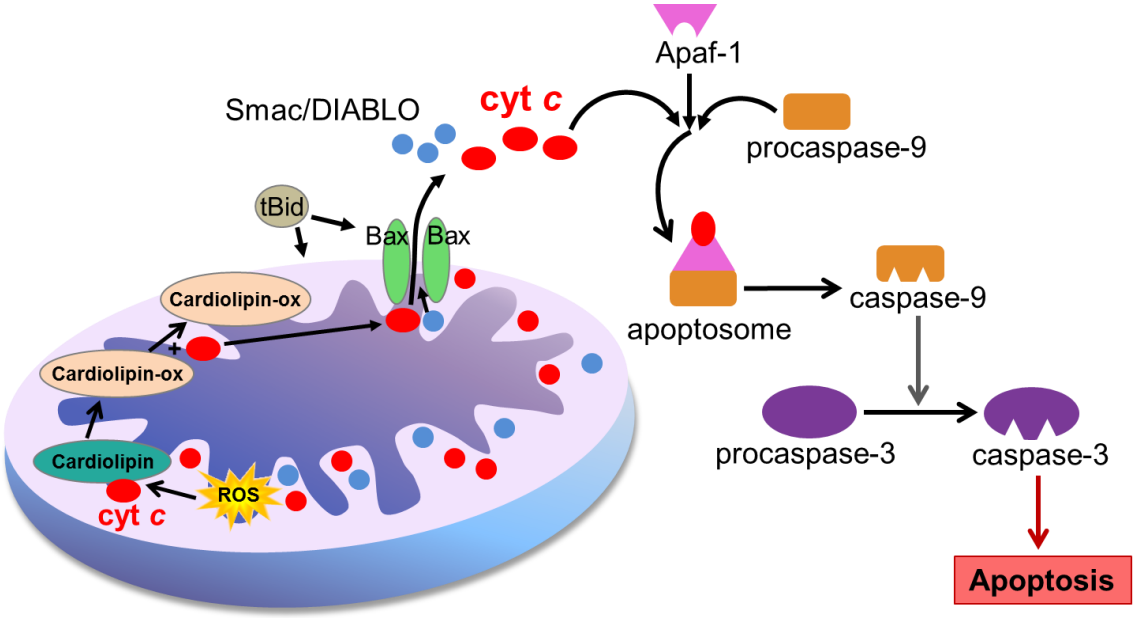

Figure 1.6. Scheme of apoptosis related to releasing of cyt *c* from mitochondrion (*6*, *19*, *21*, *22*).

1-3 Interaction of cytochrome *c* with lipids

To understand the structure-function relationship of cyt *c*, the interaction of cyt *c* with the mitochondrial membrane has been studied intensively. Cyt *c* binds to the phospholipid membrane through electrostatic interaction with the anionic head groups of phospholipids, and hydrophobic interaction with the alkyl chain moiety of phospholipids, primarily with CL (*26-29*). Electrostatic interaction between cyt *c* and the membrane has been suggested to occur initially, and in turn, induce the hydrophobic interaction between the hydrophobic cavity of cyt *c* and the acyl chain of CL (*27, 28*). Multiple lysine residues, Lys72, Lys73, Lys79, Lys86, and Lys87, on the surface of cyt

c (Figure 1.7) have been identified to be involved in the electrostatic interaction between cyt *c* and anionic phospholipids in the membrane (*27, 29-31*). The electrostatic interaction of cyt *c* with anionic phospholipids is influenced by ionic strength (*26, 27, 32-34*), membrane composition (*35*), protein-lipid ratio (*26, 36*), and the presence of other binding components such as ATP (*33, 34, 37, 38*). Hydrophobic interaction of cyt *c* with the acyl chain of phospholipids is influenced by the membrane curvature (*39*), membrane fluidity (*39, 40*), and heme oxidation state (*39, 41*).

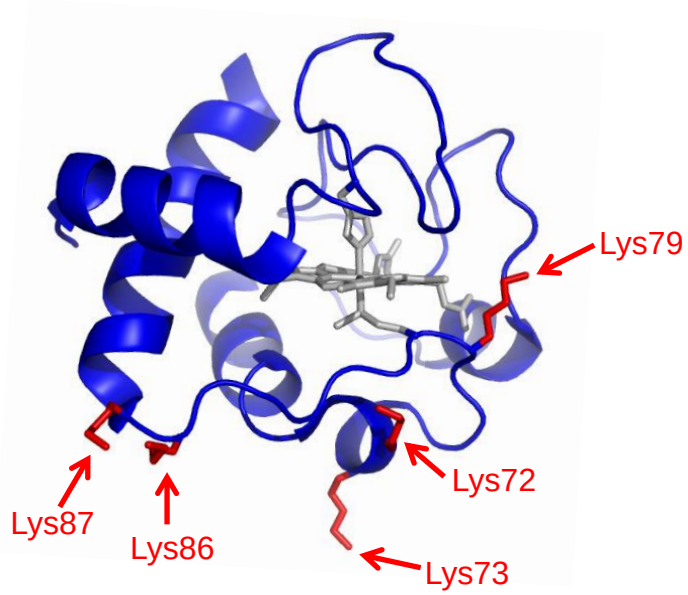

Figure 1.7. The position of Lys72, Lys73, Lys79, Lys86, and Lys87 on the surface of cyt *c* (PDB ID code:1HRC).

Cyt *c* is found to dissociate from the anionic liposomes by increasing the concentration of NaCl, $MgCl_2$, and ATP (*26, 27, 32-34*). Dissociation of cyt *c* from the CL/phosphatidylcholine (PC) and phosphatidylglycerol (PG)/PC liposomes is reduced by increasing the number of negatively charged phospholipids in the liposome (*26*). The Cl^- ion from NaCl and $MgCl_2$ compete with the negatively charged phospholipid for binding to the basic residues of cyt *c*. ATP competes with the anionic phospholipid for binding to a specific cyt *c* site, which is composed of a cluster of positively charged residues (*37, 38*). The binding strength of cyt *c* to the negatively charged phospholipids is reported to depend on the headgroup of the anionic phospholipid (*35*). Tetraoleoyl cardiolipin (TOCL) (Figure 1.8A) and dioleoyl phosphatidic acid (DOPA) (Figure 1.8B) with similar headgroups exhibited very similar binding strength. Dioleoyl phosphatidylinositol triphosphate ($DOPIP_3$) (Figure 1.8C), dioleoyl phosphatidylinositol diphosphate ($DOPIP_2$) (Figure 1.8D), and dioleoyl phosphatidylserine (DOPS) (Figure 1.8E) interact with cyt *c* more weakly compared to CL and DOPA, whereas PIP_3 interacts more strongly compared to DOPS. The difference in the binding strength can be attributed to the difference in the p*K*a value of the anionic group and the bulky head group of the phospholipid.

Hydrophobic interaction of cyt *c* with small unilamellar vesicles (SUVs) composed of PG and PC is stronger than that with large unilamellar vesicles (LUVs). SUVs may possess a larger curvature compared to LUVs, and thus expose their hydrophobic interior to the bound cyt *c* and promote hydrophobic interaction (*39*). More cyt *c* bind to the membranes in the gel phase compared to the liquid crystalline phase (*39, 40*). Since the membrane in the gel phase is less flexible than that in the liquid crystalline phase, cyt *c* in the gel phase has to adapt to the flat membrane surface to bind to the membrane, which may force cyt *c* to unfold and interact hydrophobically with the acyl chain (*39*). Oxidized cyt *c* is also found to interact more hydrophobically with the membrane compared to reduced cyt *c* (*39, 41*). Reduced cyt *c* is less positively charged and more stable than oxidized cyt *c (39)*. Therefore, oxidized cyt *c* may undergo a larger extent of unfolding and interact more hydrophobically compared to reduced cyt *c* when interacting with the liposome composed of PG and PC.

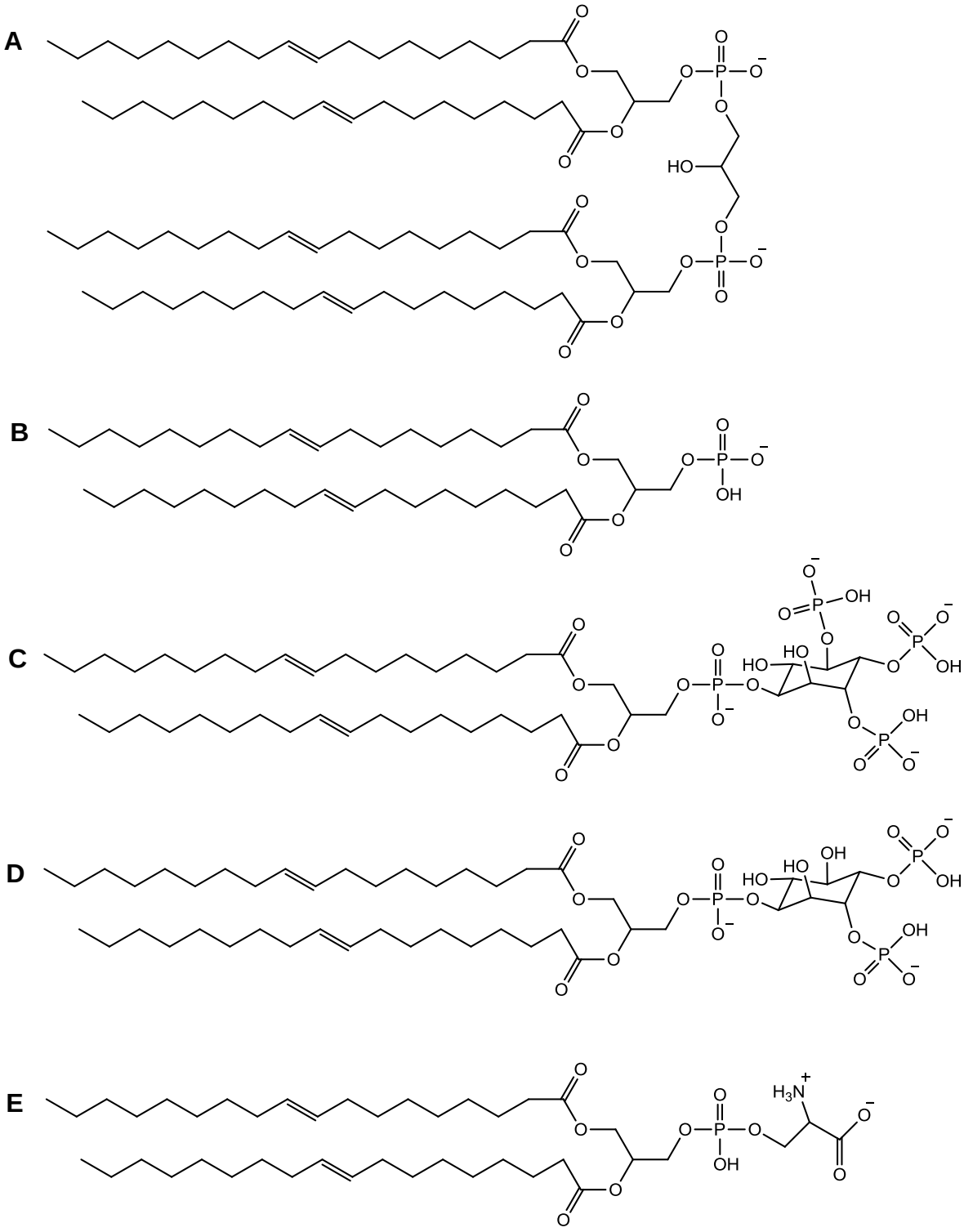

Figure 1.8. Chemical structures of (A) TOCL, (B) DOPA, (C) $DOPIP_3$, (D) $DOPIP_2$, and (E) DOPS.

1-3-1 Effects of lipids on cytochrome *c*

Interaction of cyt *c* with an anionic phospholipid-containing membrane has been shown to induce a conformational change in cyt *c* from its native state (*41*) to partially unfolded state (*42, 43*). The partially unfolded state is associated with the disruption of the tightly packed hydrophobic core of native cyt *c* (loosening of the protein tertiary structure) (*35, 44*), some alteration at the helical segment (*45*), unfolding of the C-terminal α-helical region (*46*), and releasing of the Met80 residue from the heme iron (*35, 42, 47*). The extent of the structural perturbation increased with increasing the surface density of the negatively charged phospholipid in the membrane (*44*). This structural perturbation is reported to reduce the thermal stability of cyt *c (44)*.

Under physiological ionic strength (I ~ 150 mM) and pH (7.4) conditions, multiple conformations of CL-bound cyt *c* on the membrane have been detected (*45, 46*). Cyt *c* has been found to be in an equilibrium between the free and IMM-bound states (*45*). Cortese *et al.* suggested that the initial interaction of cyt *c* with the membrane results in a surface associated state, where cyt *c* retains a native-like secondary structure with an electron transfer activity similar to that of the native soluble protein. A more deeply inserted state of cyt *c* into the membrane has been identified to be associated with a decrease in α-helical content and an increase in β-sheet content. This

membrane-inserted form exhibited an electron transfer activity less than that of the native soluble form. Bradley *et al*. also showed that both the ferric and ferrous forms of the heme of a CL-cyt *c* complex exist as multiple conformers at pH 7.4 (*48*). The heme in the ferric state of these conformers was ligated by His/Lys or His/OH^-. For the ferrous state, the heme iron takes predominantly a high-spin state with the five-coordination fashion with His.

In the presence of H_2O_2, interaction of cyt *c* with CL enhances the peroxidase activity of cyt *c* (*47*). The increase in the peroxidase activity of cyt *c* is attributed to the unligation of Met80 from the heme, to facilitate the accessibility of H_2O_2 to the heme. This is due to the hydrophobic interaction between cyt *c* and the acyl chain of CL. The CL-activated peroxidase activity of cyt *c* is reported to catalyze the oxidation of the unsaturated acyl chain of CL, producing oxidized CL which binds to cyt *c* less effectively compared to intact CL (*47, 49, 50*).

1-3-2 Effects of cytochrome *c* on lipid membranes

In anionic phospholipid-containing vesicles, cyt *c* induces reorganization of phospholipids in the membrane to form anionic phospholipid-enriched domains (*51, 52*). The lateral phase separation of the phospholipid in the presence of cyt *c* is a result of the

preferential interaction of cyt *c* with the anionic phospholipids in the membrane. The molecular interactions among the phospholipids and their lateral packing density in the anionic phospholipid-enriched domains are different from those in the zwitterionic phospholipid-enriched domains (*53*). The anionic phospholipid-enriched domains may also prefer a negative spontaneous curvature (*54*). These properties of the membrane will lead to phase boundary defects in the membrane, and leakage of vesicle substances may occur across the membrane.

Beales *et al*. found that cyt *c* binds strongly to dioleoyl phosphatidylglycerol (DOPG)- (Figure 1.9) or CL-rich domains, and observed morphological transitions within these regions of the membrane (*54*). DOPG- or CL-rich domains started to form small buds, and in turn the domains collapsed into tight, folded structures. Before collapsion, many leakages were observed from the DOPG- or CL-rich domains in the vesicles. This leakage may allow cyt *c* to bind to both the inner and the outer leaflets of the membrane. Thus, cyt *c* may induce the electrostatic attraction between the two anionic segments of the same membrane in a vesicle, in turn leading to the membrane fold and collapse.

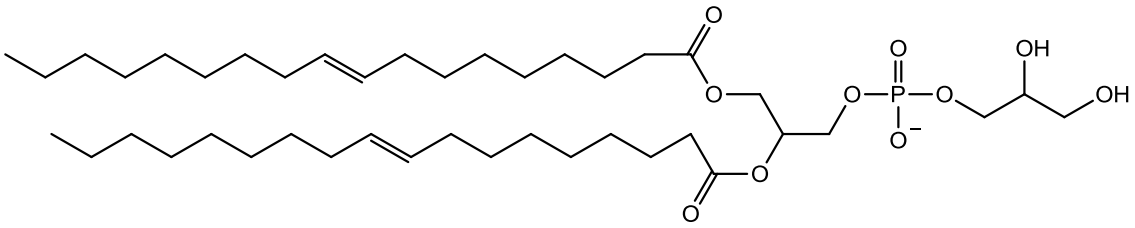

Figure 1.9. Chemical structure of DOPG.

Many researchers have proposed different mechanisms on the membrane leakage induced by the interaction of cyt *c* with an anionic phospholipid, especially CL. The binding of cyt *c* to the CL-containing membrane increases the negative curvature stress of the membrane, which then induces the hexagonal (H_{II}) phase of CL (*55*). Cyt *c* may reside within the aqueous channel (space between hydrophilic cyt *c* and phospholipids) of the H_{II} lipid structure and be released to the opposite site of the bilayer membrane (Figure 1.10). The negative curvature stress is also suggested to induce formation of a toroidal pore, which is stabilized by the unfolded C-terminal helix of cyt *c* (*56*). The pore formation through a "carpet" mechanism also might be induced by the interaction of cyt *c* with the membranes (*36*). In the "carpet" mechanism, protein initially binds electrostatically to the anionic head group of the phospholipid on the surface of the membrane, following with reorientation of the hydrophobic residues of the protein toward the hydrophobic core of the membrane (*57*). Membrane-bound

proteins cover the membrane in a carpet-like manner and generate high surface pressure to the membrane at high surface protein concentrations (*57, 58*). At a critical concentration threshold, this pressure may become high enough for the formation of transient pores in the membrane.

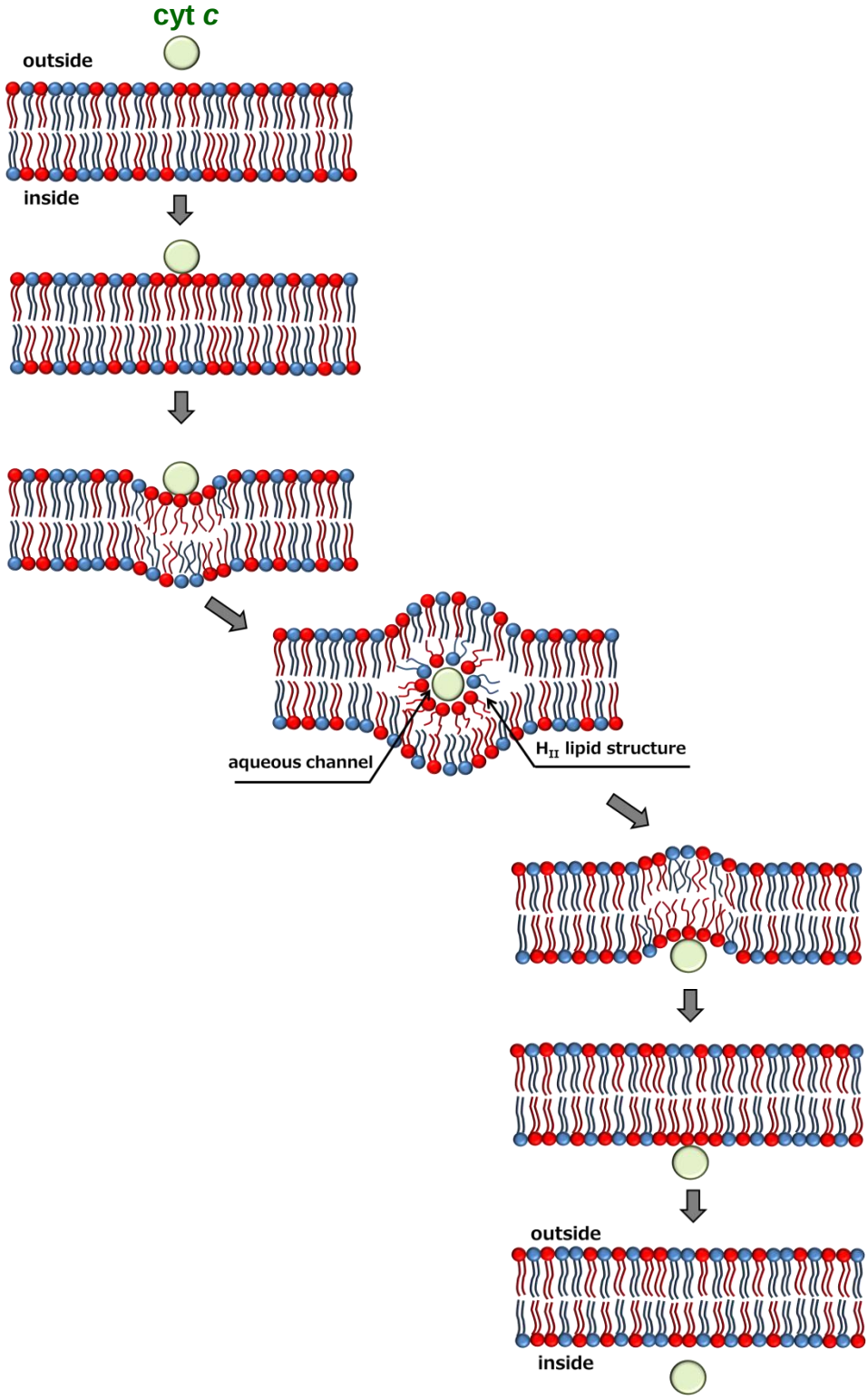

Figure 1.10. Schematic representation of the formation of hexagonal (H_{II}) lipid structure by cyt *c* in the CL-containing bilayer. The lipids with the red and blue head-groups represent CL and the zwitterionic phospholipid, respectively. Cyt *c* is depicted as a green sphere (*55*).

1-4 Purpose of this study

Monomeric cyt *c* was found to bind to the mitochondrial membrane through electrostatic and hydrophobic interactions with anionic phospholipids, especially CL. This interaction induces a conformational change in native cyt *c* and a morphological change in the lipid membrane, which in turn may control the function of cyt *c* in the respiratory chain and trigger the release of cyt *c* from the mitochondrial membrane at the early stage of apoptosis. Domain-swapped oligomeric cyt *c* has been reported to maintain the secondary structures of the monomer, whereas its surface possesses a larger area and more charges compared to the monomer (Figure 1.11). Therefore, I envisaged that the domain-swapped oligomeric cyt *c* may bind more strongly to the anionic phospholipid and induce more morphological changes in lipid membranes compared to the monomer.

Although the biological functions of monomeric cyt *c* have been studied intensively, the effect of oligomerization of cyt *c* on cells is as yet unrevealed. Therefore, in this study, the interaction of domain-swapped oligomeric cyt *c* with negatively charged liposomes and cell membranes was investigated in order to understand the biological properties of domain-swapped oligomeric cyt *c*.

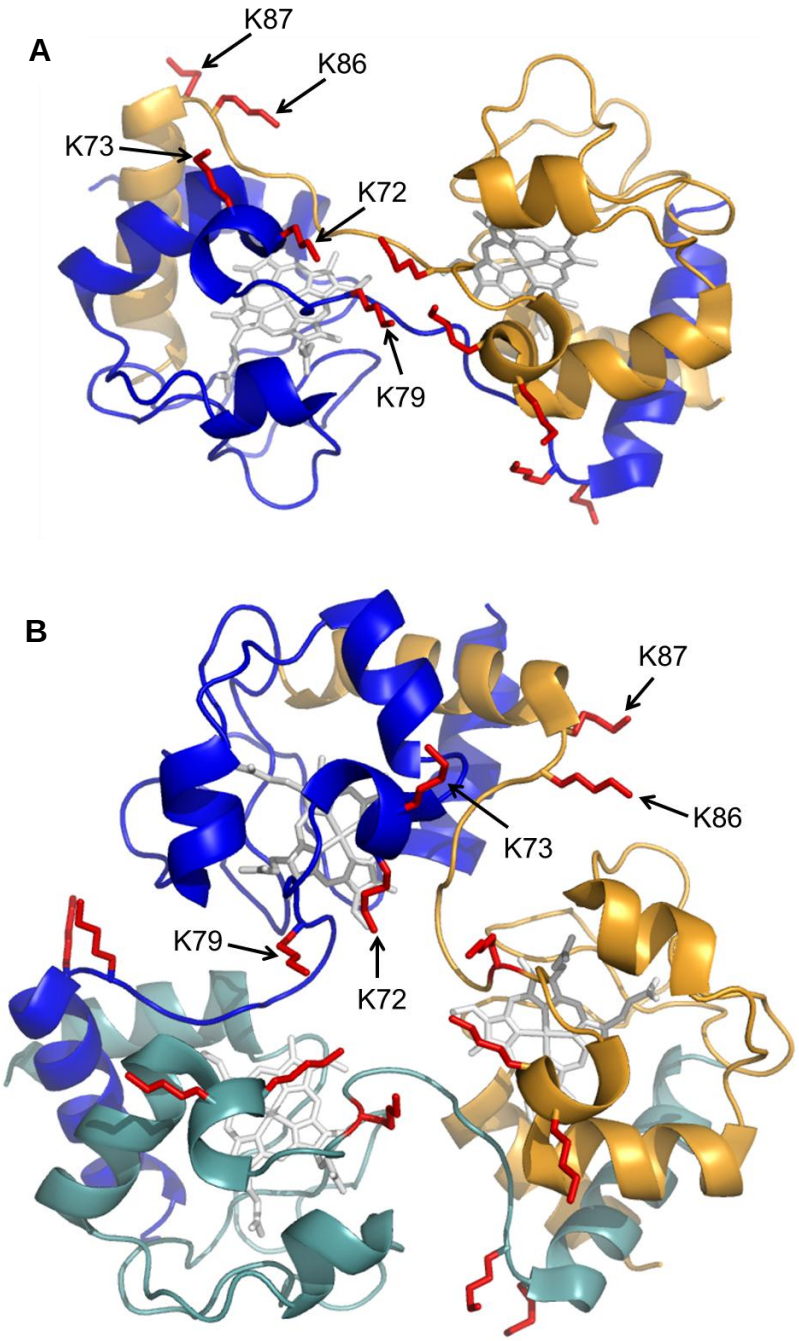

Figure 1.11. Structures of (A) dimeric (PDB ID code:3NBS) and (B) trimeric (PDB ID code:3NBT) horse cyt *c*. Side-chain atoms of Lys72, Lys73, Lys79, Lys86, and Lys87 are shown as red stick models.

1-5 References

1. Alberts, B., Bray, D., Hopkin, K., Johnson, A., Lewis, J., Raff, M., Roberts, K., and Walter, P. (2010) *Essential cell biology*, third ed., Garland Science, New York.

2. Alberts, B., Johnson, A., Lewis, J., Raff, M., Roberts, K., and Walter, P. (2008) *Molecular biology of the cell*, fifth ed., Garland Science, New York.

3. Karp, G. (1996) *Cell and molecular biology: concepts and experiments*, John Wiley & Sons, New York.

4. Chen, L. B. (1988) Mitochondrial membrane potential in living cells, *Annu. Rev. Cell Biol. 4*, 155-181.

5. McBride, H. M., Neuspiel, M., and Wasiak, S. (2006) Mitochondria: more than just a powerhouse, *Curr. Biol. 16*, R551-560.

6. Saelens, X., Festjens, N., Vande Walle, L., van Gurp, M., van Loo, G., and Vandenabeele, P. (2004) Toxic proteins released from mitochondria in cell death, *Oncogene 23*, 2861-2874.

7. Dickerson, R. E., Takano, T., Eisenberg, D., Kallai, O. B., Samson, L., Cooper, A., and Margoliash, E. (1971) Ferricytochrome *c*. I. General features of the horse and bonito proteins at 2.8 A resolution, *J. Biol. Chem. 246*, 1511-1535.

8. Bushnell, G. W., Louie, G. V., and Brayer, G. D. (1990) High-resolution three-dimensional structure of horse heart cytochrome *c*, *J. Mol. Biol. 214*, 585-595.

9. Barlow, G. H., and Margoliash, E. (1966) Electrophoretic behavior of mammalian-type cytochromes *c*, *J. Biol. Chem. 241*, 1473-1477.

10. Margalit, R., and Schejter, A. (1973) Cytochrome *c*: a thermodynamic study of relationships among oxidation state, ion-binding and structural parameters. 2. Ion-binding linked to oxidation state, *Eur. J. Biochem. 32*, 500-505.

11. Atwood, J. L., Davies, J. E. D., Macnicol, D. D., and Vögtle, F. (1996) *Comprehensive supramolecular chemistry*, Vol. 5, Pergamon Press, Oxford, UK.

12. Hirota, S., Hattori, Y., Nagao, S., Taketa, M., Komori, H., Kamikubo, H., Wang, Z., Takahashi, I., Negi, S., Sugiura, Y., Kataoka, M., and Higuchi, Y. (2010) Cytochrome *c* polymerization by successive domain swapping at the C-terminal helix, *Proc. Natl. Acad. Sci. U. S. A. 107*, 12854-12859.

13. Ott, M., Robertson, J. D., Gogvadze, V., Zhivotovsky, B., and Orrenius, S. (2002) Cytochrome *c* release from mitochondria proceeds by a two-step process, *Proc. Natl. Acad. Sci. U. S. A. 99*, 1259-1263.

14. Huttemann, M., Pecina, P., Rainbolt, M., Sanderson, T. H., Kagan, V. E.,

Samavati, L., Doan, J. W., and Lee, I. (2011) The multiple functions of cytochrome *c* and their regulation in life and death decisions of the mammalian cell: From respiration to apoptosis, *Mitochondrion 11*, 369-381.

15. Tollin, G., Hanson, L. K., Caffrey, M., Meyer, T. E., and Cusanovich, M. A. (1986) Redox pathways in electron-transfer proteins: correlations between reactivities, solvent exposure, and unpaired-spin-density distributions, *Proc. Natl. Acad. Sci. U. S. A. 83*, 3693-3697.

16. Arnold, S., and Kadenbach, B. (1999) The intramitochondrial ATP/ADP-ratio controls cytochrome *c* oxidase activity allosterically, *FEBS Lett. 443*, 105-108.

17. Lee, I., Salomon, A. R., Yu, K., Doan, J. W., Grossman, L. I., and Huttemann, M. (2006) New prospects for an old enzyme: mammalian cytochrome *c* is tyrosine-phosphorylated in vivo, *Biochemistry 45*, 9121-9128.

18. Yu, H., Lee, I., Salomon, A. R., Yu, K., and Huttemann, M. (2008) Mammalian liver cytochrome *c* is tyrosine-48 phosphorylated in vivo, inhibiting mitochondrial respiration, *Biochim. Biophys. Acta 1777*, 1066-1071.

19. Liu, X., Kim, C. N., Yang, J., Jemmerson, R., and Wang, X. (1996) Induction of apoptotic program in cell-free extracts: requirement for dATP and cytochrome *c*, *Cell 86*, 147-157.

20. Robertson, J. D., Orrenius, S., and Zhivotovsky, B. (2000) Review: nuclear events in apoptosis, *J. Struct. Biol. 129*, 346-358.

21. Kagan, V. E., Tyurin, V. A., Jiang, J., Tyurina, Y. Y., Ritov, V. B., Amoscato, A. A., Osipov, A. N., Belikova, N. A., Kapralov, A. A., Kini, V., Vlasova, II, Zhao, Q., Zou, M., Di, P., Svistunenko, D. A., Kurnikov, I. V., and Borisenko, G. G. (2005) Cytochrome *c* acts as a cardiolipin oxygenase required for release of proapoptotic factors, *Nat. Chem. Biol. 1*, 223-232.

22. Orrenius, S., and Zhivotovsky, B. (2005) Cardiolipin oxidation sets cytochrome *c* free, *Nat. Chem. Biol. 1*, 188-189.

23. Ow, Y. P., Green, D. R., Hao, Z., and Mak, T. W. (2008) Cytochrome *c*: functions beyond respiration, *Nat. Rev. Mol. Cell Biol. 9*, 532-542.

24. Kroemer, G., Galluzzi, L., and Brenner, C. (2007) Mitochondrial membrane permeabilization in cell death, *Physiol. Rev. 87*, 99-163.

25. Annis, M. G., Soucie, E. L., Dlugosz, P. J., Cruz-Aguado, J. A., Penn, L. Z., Leber, B., and Andrews, D. W. (2005) Bax forms multispanning monomers that oligomerize to permeabilize membranes during apoptosis, *EMBO J. 24*, 2096-2103.

26. Rytomaa, M., and Kinnunen, P. K. (1994) Evidence for two distinct acidic

phospholipid-binding sites in cytochrome *c*, *J. Biol. Chem. 269*, 1770-1774.

27. Rytomaa, M., and Kinnunen, P. K. (1995) Reversibility of the binding of cytochrome *c* to liposomes. Implications for lipid-protein interactions, *J. Biol. Chem. 270*, 3197-3202.

28. Kalanxhi, E., and Wallace, C. J. (2007) Cytochrome *c* impaled: investigation of the extended lipid anchorage of a soluble protein to mitochondrial membrane models, *Biochem. J. 407*, 179-187.

29. Sinibaldi, F., Howes, B. D., Piro, M. C., Polticelli, F., Bombelli, C., Ferri, T., Coletta, M., Smulevich, G., and Santucci, R. (2010) Extended cardiolipin anchorage to cytochrome *c*: a model for protein-mitochondrial membrane binding, *J. Biol. Inorg. Chem. 15*, 689-700.

30. Kostrzewa, A., Pali, T., Froncisz, W., and Marsh, D. (2000) Membrane location of spin-labeled cytochrome *c* determined by paramagnetic relaxation agents, *Biochemistry 39*, 6066-6074.

31. Sinibaldi, F., Howes, B. D., Droghetti, E., Polticelli, F., Piro, M. C., Di Pierro, D., Fiorucci, L., Coletta, M., Smulevich, G., and Santucci, R. (2013) Role of lysines in cytochrome *c*-cardiolipin interaction, *Biochemistry 52*, 4578-4588.

32. Sinibaldi, F., Fiorucci, L., Patriarca, A., Lauceri, R., Ferri, T., Coletta, M., and

Santucci, R. (2008) Insights into cytochrome *c*-cardiolipin interaction. Role played by ionic strength, *Biochemistry 47*, 6928-6935.

33. Sinibaldi, F., Droghetti, E., Polticelli, F., Piro, M. C., Di Pierro, D., Ferri, T., Smulevich, G., and Santucci, R. (2011) The effects of ATP and sodium chloride on the cytochrome *c*-cardiolipin interaction: the contrasting behavior of the horse heart and yeast proteins, *J. Inorg. Biochem. 105*, 1365-1372.

34. Rytomaa, M., Mustonen, P., and Kinnunen, P. K. (1992) Reversible, nonionic, and pH-dependent association of cytochrome *c* with cardiolipin-phosphatidylcholine liposomes, *J. Biol. Chem. 267*, 22243-22248.

35. Kapralov, A. A., Kurnikov, I. V., Vlasova, II, Belikova, N. A., Tyurin, V. A., Basova, L. V., Zhao, Q., Tyurina, Y. Y., Jiang, J., Bayir, H., Vladimirov, Y. A., and Kagan, V. E. (2007) The hierarchy of structural transitions induced in cytochrome *c* by anionic phospholipids determines its peroxidase activation and selective peroxidation during apoptosis in cells, *Biochemistry 46*, 14232-14244.

36. Oellerich, S., Lecomte, S., Paternostre, M., Heimburg, T., and Hildebrandt, P. (2004) Peripheral and integral binding of cytochrome *c* to phospholipids vesicles, *J. Phys. Chem. B 108*, 3871-3878.

37. Sinibaldi, F., Mei, G., Polticelli, F., Piro, M. C., Howes, B. D., Smulevich, G.,

Santucci, R., Ascoli, F., and Fiorucci, L. (2005) ATP specifically drives refolding of non-native conformations of cytochrome *c*, *Protein Sci. 14*, 1049-1058.

38. Tuominen, E. K., Zhu, K., Wallace, C. J., Clark-Lewis, I., Craig, D. B., Rytomaa, M., and Kinnunen, P. K. (2001) ATP induces a conformational change in lipid-bound cytochrome *c*, *J. Biol. Chem. 276*, 19356-19362.

39. Kim, U., Kim, Y. S., and Han, S. (2000) Modulation of cytochrome *c*-membrane interaction by physical state of the membrane and the redox state of cytochrome *c*, *Bull. Korean Chem. Soc. 21*, 412-418.

40. Hamachi, I., Fujita, A., and Kunitake, T. (1997) Protein engineering using molecular assembly: functional conversion of cytochrome *c* via noncovalent interactions, *J. Am. Chem. Soc. 119*, 9096-9102.

41. Bernabeu, A., Contreras, L. M., and Villalain, J. (2007) Two-dimensional infrared correlation spectroscopy study of the interaction of oxidized and reduced cytochrome *c* with phospholipid model membranes, *Biochim. Biophys. Acta 1768*, 2409-2420.

42. Sanghera, N., and Pinheiro, T. J. (2000) Unfolding and refolding of cytochrome *c* driven by the interaction with lipid micelles, *Protein Sci. 9*, 1194-1202.

43. Pinheiro, T. J., Elove, G. A., Watts, A., and Roder, H. (1997) Structural and

kinetic description of cytochrome *c* unfolding induced by the interaction with lipid vesicles, *Biochemistry 36*, 13122-13132.

44. Muga, A., Mantsch, H. H., and Surewicz, W. K. (1991) Membrane binding induces destabilization of cytochrome *c* structure, *Biochemistry 30*, 7219-7224.

45. Cortese, J. D., Voglino, A. L., and Hackenbrock, C. R. (1998) Multiple conformations of physiological membrane-bound cytochrome *c*, *Biochemistry 37*, 6402-6409.

46. Hanske, J., Toffey, J. R., Morenz, A. M., Bonilla, A. J., Schiavoni, K. H., and Pletneva, E. V. (2012) Conformational properties of cardiolipin-bound cytochrome *c*, *Proc. Natl. Acad. Sci. U. S. A. 109*, 125-130.

47. Vladimirov, Y. A., Proskurnina, E. V., Izmailov, D. Y., Novikov, A. A., Brusnichkin, A. V., Osipov, A. N., and Kagan, V. E. (2006) Mechanism of activation of cytochrome *c* peroxidase activity by cardiolipin, *Biochemistry (Moscow) 71*, 989-997.

48. Bradley, J. M., Silkstone, G., Wilson, M. T., Cheesman, M. R., and Butt, J. N. (2011) Probing a complex of cytochrome *c* and cardiolipin by magnetic circular dichroism spectroscopy: implications for the initial events in apoptosis, *J. Am. Chem. Soc. 133*, 19676-19679.

49. Shidoji, Y., Hayashi, K., Komura, S., Ohishi, N., and Yagi, K. (1999) Loss of molecular interaction between cytochrome *c* and cardiolipin due to lipid peroxidation, *Biochem. Biophys. Res. Commun. 264*, 343-347.

50. Tyurina, Y. Y., Kini, V., Tyurin, V. A., Vlasova, II, Jiang, J., Kapralov, A. A., Belikova, N. A., Yalowich, J. C., Kurnikov, I. V., and Kagan, V. E. (2006) Mechanisms of cardiolipin oxidation by cytochrome *c*: relevance to pro- and antiapoptotic functions of etoposide, *Mol. Pharmacol. 70*, 706-717.

51. Brown, L. R., and Wuthrich, K. (1977) NMR and ESR studies of the interactions of cytochrome *c* with mixed cardiolipin-phosphatidylcholine vesicles, *Biochim. Biophys. Acta 468*, 389-410.

52. Haverstick, D. M., and Glaser, M. (1989) Influence of proteins on the reorganization of phospholipid bilayers into large domains, *Biophys. J. 55*, 677-682.

53. Epand, R. M., and Epand, R. F. (2009) Lipid domains in bacterial membranes and the action of antimicrobial agents, *Biochim. Biophys. Acta 1788*, 289-294.

54. Beales, P. A., Bergstrom, C. L., Geerts, N., Groves, J. T., and Vanderlick, T. K. (2011) Single vesicle observations of the cardiolipin-cytochrome *c* interaction: induction of membrane morphology changes, *Langmuir 27*, 6107-6115.

55. de Kruijff, B., and Cullis, P. R. (1980) Cytochrome *c* specifically induces non-bilayer structures in cardiolipin-containing model membranes, *Biochim. Biophys. Acta 602*, 477-490.

56. Bergstrom, C. L., Beales, P. A., Lv, Y., Vanderlick, T. K., and Groves, J. T. (2013) Cytochrome *c* causes pore formation in cardiolipin-containing membranes, *Proc. Natl. Acad. Sci. U. S. A. 110*, 6269-6274.

57. Shai, Y. (1999) Mechanism of the binding, insertion and destabilization of phospholipid bilayer membranes by alpha-helical antimicrobial and cell non-selective membrane-lytic peptides, *Biochim. Biophys. Acta 1462*, 55-70.

58. Zuckermann, M. J., and Heimburg, T. (2001) Insertion and pore formation driven by adsorption of proteins onto lipid bilayer membrane-water interfaces, *Biophys. J. 81*, 2458-2472.

Chapter 2

Morphological change of vesicle membrane

2-1 Introduction

Cyt *c* is a hemoprotein, transferring electrons in the mitochondrial respiratory chain and binding to Apaf-1 in the apoptotic pathway (*1-3*). Cyt *c* is bound to the inner membrane in the mitochondrial intermembrane space, and released to cytoplasm at the early stage of apoptosis. The surface of native cyt *c* is positively charged, whereas many hydrophobic contacts exist inside it (*4*, *5*). Cyt *c* binds to the mitochondrial membrane through electrostatic and hydrophobic interactions with negatively charged phospholipids, especially with CL (*6-9*). Lys72, Lys73, Lys79, Lys86, and Lys87, on the surface of cyt *c*, are reported to participate in the electrostatic binding of cyt *c* to the negatively charged phospholipids in the membrane (*7*, *9-11*). Hanske *et al.* have reported that the electrostatic interaction of cyt *c* with the negatively charged CL in the membrane unfolds the C-terminal α-helical region of cyt *c*, assisting formation of further hydrophobic contacts with the lipids (*12*). Cyt *c* retains some of its secondary structure and adopts a loosely packed tertiary structure upon binding to an anionic-lipid membrane (*13*). It has been reported that the Met80−heme iron bond of cyt *c* is cleaved by interaction with a CL-containing membrane, initiating CL peroxidation and mitochondrial permeabilization (*14-16*). The peroxidase activity of cyt *c* has also been

shown to increase on interaction with detergents (*17*) as well as for its domain-swapped dimer (*18*), owing to the dissociation of Met80 from the heme iron.

The coverage of the surface of the DOPG vesicle with cyt *c* has been reported to induce flocculation and sedimentation of the vesicle (Figure 2.1) (*19*). The flocculation and sedimentation have been attributed to the interaction between vesicles due to cyt *c* binding to the vesicles. Laterally segregated domains enriched in negatively charged phospholipids were shown to form in CL-containing liposomes by interaction with cyt *c* (*20, 21*). Also, cyt *c* induced morphological transition in liposomes containing DOPG and CL by interacting with the DOPG- and CL-rich domains, where the negatively charged domains formed small buds and eventually folded into a collapse state (*22*). It has also been suggested that cyt *c* penetrates through CL-containing vesicles by forming pores (*23*).

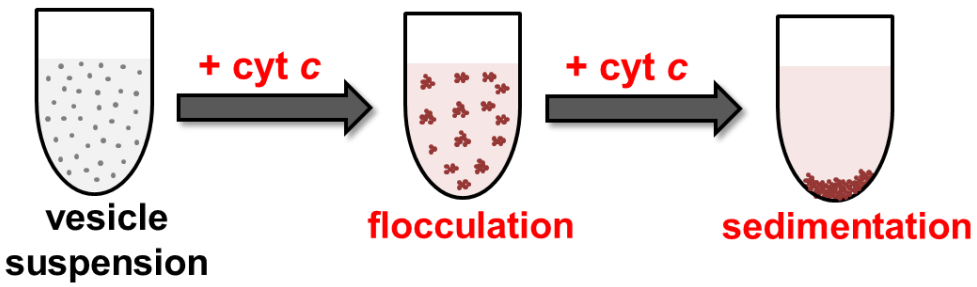

Figure 2.1. Schematic diagram of flocculation and sedimentation of vesicles in the presence of cyt *c*.

Monomeric cyt *c* has been found to form oligomers by swapping the C-terminal helix successively (*24*). Domain-swapped oligomeric cyt *c* retains secondary structures, but the surface is larger area and has more charge than the monomer. I envisaged that oligomerization of cyt *c* may induce strong binding of cyt *c* to the vesicle membrane. In this study, the interaction of domain-swapped oligomeric cyt *c* with negatively charged liposomes and its effect on the morphological change of liposomes were investigated.

2-2 Materials and methods

2-2-1 Preparation of domain-swapped oligomeric cyt *c*

Cyt *c* from horse heart was obtained from Sigma-Aldrich (St. Louis, MO, USA). Human cyt *c* was obtained by expression of recombinant human cyt *c* in *E. coli* Rosetta 2 (DE3) pLysS cells (Novagen, San Diego, CA, USA). The expression and purification of recombinant human cyt *c* were performed according to the published method (*25*). Purified human cyt *c* was oxidized by an addition of potassium ferricyanide (Wako, Osaka, Japan) (50 equivalents to the heme cofactor) to the cyt *c* solution. Potassium ferricyanide was removed subsequently from the cyt *c* solution using a DE52 (Whatman, UK) column with 50 mM potassium phosphate buffer, pH 7.0. Domain-swapped oligomeric ferric horse cyt *c* was obtained by dissolving 25 mg of horse cyt *c* in 2 mL of 50 mM potassium phosphate buffer, pH 7.0, followed by an addition of ethanol up to 60% (v/v) to the cyt *c* solution (*24*). Domain-swapped oligomeric ferric human cyt *c* was obtained by addition of ethanol to 1 mM human cyt *c* in the same buffer (final ethanol concentration, 60% (v/v)). Precipitated cyt *c* was collected by centrifugation at 9,000 g for 5 min at 4ºC, and freeze-dried. The freeze-dried powder was dissolved in 2 mL of 50 mM potassium phosphate buffer, pH 7.0. After incubation at 37ºC for 1 h, the cyt *c* solution was filtrated (Millipore, Billerica, MA, USA; pore size 0.45 μm) and

purified with gel chromatography (Hiload 26/60 Superdex 75, GE healthcare, Buckinghamshire, England) using a FPLC system (BioLogic DuoFlow 10, Bio-Rad, Hercules, CA, USA) monitored at 409 and 280 nm, with the same buffer at 4ºC. Domain-swapped dimeric, trimeric, tetrameric, octameric (average molecular weight 95 kDa) and dodecameric (average molecular weight, 145 kDa) ferric horse and human cyt *c* were collected. Absorption spectra of the monomer and oligomer were measured to confirm oxidation of cyt *c* and determine its concentration (*24*). The concentration of the cyt *c* monomer and each oligomer solution was adjusted with the Soret band intensity. The peaks of dimeric, trimeric, and tetrameric horse cyt *c* in the elution curve have been determined in the previous study (*24*). The average molecular weight of octameric and dodecameric horse cyt *c* was determined using size exclusion chromatography (Superdex 200 10/300 GL, GE healthcare). The column was calibrated with globular protein standards of ovalbumin (44 kDa; Sigma-Aldrich), conalbumin (75 kDa; Sigma-Aldrich), aldolase (158 kDa; Wako), and ferritin (440 kDa; Sigma-Aldrich), which were loaded individually on the column and monitored at 280 nm. The log of molecular weight (log MW) for each standard protein was plotted against its distribution coefficient (K_{av}), which was derived using the formula $K_{av}=(V_e-V_o)/(V_c-V_o)$, where V_e is the elution volume of the protein; V_c is the total liquid volume of the

column; and V_o is the void volume of the column, which was determined from the elution volume of blue dextran. K_{av} of the two fractions was calculated, and interpolated on the calibration curve (log MW *vs* K_{av}) to determine the average molecular weight of the proteins in the fractions.

2-2-2 LUVs formation

The formation of LUVs was conducted according to the previous protocol (*26*) with modifications. 1,2-dipalmitoyl-*sn*-glycero-3-phosphoglycerol (DPPG, NOF Co., Tokyo, Japan) (Figure 2.2A) and 1,2-dimyristoyl-*sn*-glycero-3-phosphocholine (DMPC, NOF Co.) (Figure 2.2B) were dissolved separately in chloroform/methanol (5:1 (v/v)). Both lipids were mixed with same stoichiometry for preparation of DPPG/DMPC (1:1) vesicles, whereas the DMPC solution was used without DPPG for preparation of DMPC vesicles. The lipid solution was dried with a rotary evaporator at 50ºC to deposit lipids as a film on the wall of a round-bottom flask. The obtained lipid films were suspended in 25 mM HEPES-NaOH buffer, pH 7.4, containing 10 mM NaCl, and incubated at 55ºC for 3 min followed by vigorous mixing by vortex for 3 min. The vesicle suspension was frozen subsequently with liquid nitrogen, and incubated at 55ºC for 3 min. After repeating the vortexing, freezing and heating four times, the vesicle

suspension was separated into several flasks and stored at -80ºC until used. Before use, the vesicle suspension was heated at 55ºC for 3 min and subsequently vortexed for 3 min, and passed through a 100 nm polycarbonate membrane at 50ºC using a LiposoFast-Extruder (Avestin, Ottawa, ON, Canada) to adjust the size.

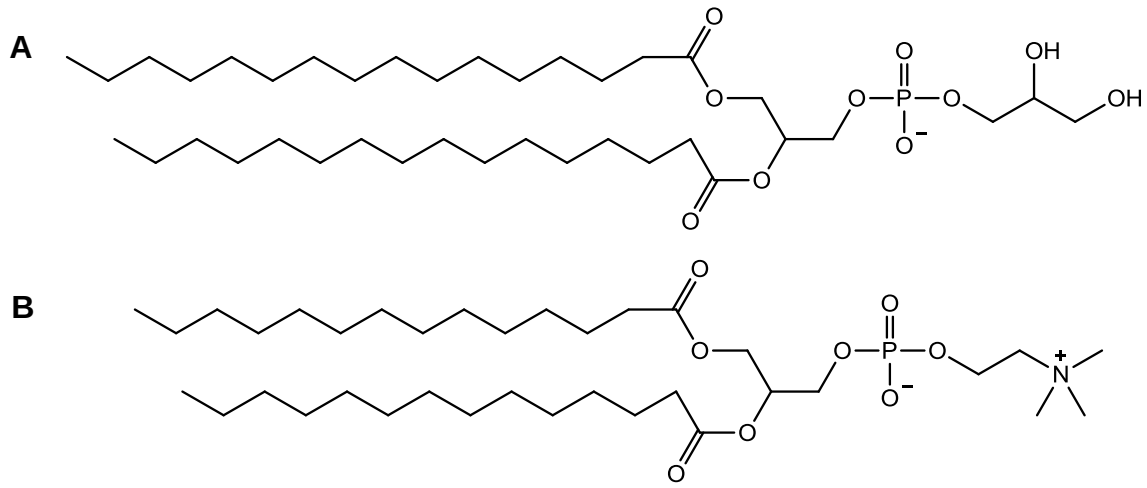

Figure 2.2. Chemical structures of (A) DPPG and (B) DMPC

2-2-3 Analysis of interaction between cyt *c* and LUV

A DPPG/DMPC (1:1) or DMPC LUV stock solution was diluted with 25 mM HEPES-NaOH buffer, pH 7.4, containing 10, 50, 100, 150, 200, or 400 mM NaCl. The absorption spectra of monomeric, dimeric, trimeric, tetrameric, and dodecameric ferric cyt *c* from horse and human in the same buffer were measured with a UV-2450 spectrophotometer (Shimadzu, Tokyo, Japan). Horse or human cyt *c* solution was added

to the LUV solution. Final concentrations of the lipid and heme were 1 mM and 25 μM, respectively. The mixture of LUV and monomeric, dimeric, trimeric, tetrameric or dodecameric cyt *c* was incubated at 20ºC for 1.5 h, and centrifuged at 5000 g for 5 min at 20ºC. The supernatant was collected, and the absorption spectrum was measured at 20ºC with the UV-2450 spectrophotometer. The difference in the absorbance at 409 and 371 nm (for monomeric cyt *c*) or that at 407 and 366 nm (for oligomeric cyt *c*) was calculated in order to omit the absorbance of lipids. The percentage of cyt *c* in the supernatant was obtained by dividing the absorbance difference after the incubation with that before the incubation, and multiplying the obtained value with 100. The percentage of cyt *c* precipitates was calculated by subtracting the percentage of cyt *c* in the supernatant from 100. For the analysis of the interaction between horse cyt *c* and DMPC LUVs, the absorbance of the DMPC LUV solution was subtracted from that of horse cyt *c* after incubation with DMPC LUVs.

2-2-4 Differential scanning calorimetry (DSC) measurement

DSC measurements were performed with VP-DSC (Microcal, GE Healthcare). The scan rate was 1ºC/min over the temperature range 5−55ºC. Suspension of DPPG/DMPC (1:1) LUV was mixed with monomeric, domain-swapped dimeric, or

dodecameric ferric horse cyt *c* in 25 mM HEPES-NaOH buffer, pH 7.4, containing 10 mM NaCl. The final concentrations of the lipid and heme were 1 mM and 25 μM, respectively. The mixed solution was incubated at 20ºC for 1.5 h. After the incubation, the sample was loaded to the calorimeter cell at temperatures below 15ºC.

2-2-5 GUV formation

Giant unilamellar vesicles (GUVs, ≥1 μm in diameter) were formed with electroformation (Figure 2.3). DPPG and DMPC stock solutions in chloroform/methanol (5:1 (v/v)) were mixed at molar ratio of DPPG:DMPC=1:1. *N*-(lissamine rhodamine B)-1,2-dihexadecanoyl-*sn*-glycero-3-phosphoethanolamine, triethylammonium salt (*N*-Rh-PE, Molecular Probes, Eugene, OR, USA) was added to the lipid solution (final concentration, 1 mol%). The final concentration of the lipid in chloroform/methanol (5:1 (v/v)) was 0.5 mg/ml. The lipid solution (10 μl) was placed drop wise on an indium tin oxide (ITO)-coated slide, and dried with N_2 gas to form a thin lipid film. The ITO-coated slide was heated above 45ºC to obtain a fluid phase for the lipids. The electroformation chamber was placed on the ITO-coated slide with the lipids, and filled with 400 μl pure water. The chamber was covered with another ITO-coated slide, and 4.0 V alternating current electric field was applied across the

ITO-coated slides at 10 Hz for about 30 min. The temperature of the chamber was monitored with a digital surface thermometer HFT-50 (Anritsu, Tokyo, Japan), and adjusted to 43ºC.

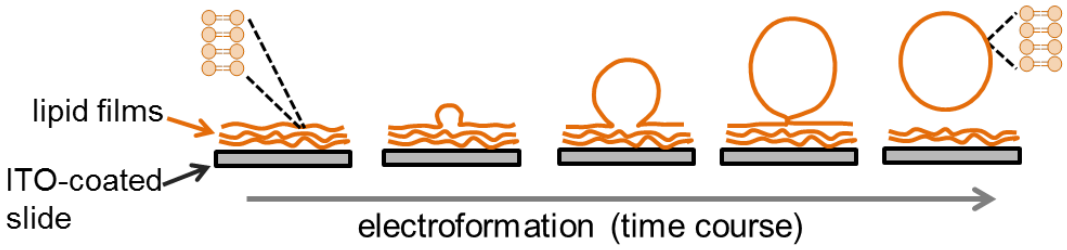

Figure 2.3. Schematic diagram of GUV formation with electroformation.

2-2-6 Fluorescence microscopy

GUVs were imaged using an Olympus IX71 microscope (Olympus, Center Valley, PA, USA). An Olympus 60x/1.4 N.A Plan Apo differential interference contrast oil immersion objective lens was used. Excitation light from a Hg lamp was irradiated with a U-MWIG2 filter set (dichromatic mirror; excitation wavelength, 520–550 nm; cut-on wavelength 565 nm) (Olympus, Center Valley, PA, USA). Monomeric, domain-swapped dimeric, and domain-swapped dodecameric ferric horse cyt *c* (200 μM heme, 1 μl) in 25 mM HEPES-NaOH buffer, pH 7.4, containing 10 mM NaCl was injected slowly near the monitoring GUV in pure water (final concentration of horse cyt *c*, 0.5 μM heme). GUV was monitored at 43ºC for 12 min.

2-3 Results and discussion

In this study, the binding behaviour of domain-swapped oligomeric cyt *c* to lipid membranes was investigated with LUVs composed of negatively charged 1,2-dipalmitoyl-*sn*-glycero-3-phosphoglycerol (DPPG) and zwitterionic 1,2-dimyristoyl-*sn*-glycero-3-phosphocholine (DMPC) (DPPG:DMPC=1:1) or only DMPC. The size of the LUVs was adjusted to ~100 nm in diameter. Oligomeric ferric horse cyt *c* was obtained by treatment with ethanol as previously reported (*24*), and subsequently purified with gel chromatography (Figure 2.4). The average molecular weight of octameric and dodecameric horse cyt *c* was determined by interpolating its K_{av} on the calibration curve of the Superdex 200 column (Figure 2.5). Precipitates were formed by incubation of DPPG/DMPC (1:1) LUV dispersion (1 mM total lipids) with monomeric or oligomeric horse ferric cyt *c* (25 μM heme) (Figure 2.6). The amount of precipitates increased by incubation with oligomeric cyt *c* compared to monomeric cyt *c*. However, precipitates were not detected when oligomeric horse cyt *c* was added to DMPC LUVs without negatively charged DPPG. To investigate the interaction of cyt *c* and LUV in more detail, the precipitate in each suspension was estimated from the amount of cyt *c* remaining in the solution after incubation (Figures 2.7 and 2.8, Table A.1, A.2 and A.3). The amount of cyt *c* precipitated by interaction with LUV increased

with increase in the order of cyt *c* oligomers (Figure 2.7A and Table A.1), and decreased with increase in the NaCl concentration from 10 to 400 mM in the solution (Figures 2.6 and 2.8). The amount of monomeric, dimeric, and dodecameric cyt *c* precipitated by incubation with DPPG/DMPC (1:1) LUVs was 5%, 6%, and 7% (Figure 2.8 and Table A.3), respectively, in the presence of 400 mM NaCl. These results show that electrostatic interaction plays an important role for horse cyt *c* in the interaction of the monomer or oligomer with the lipids. Oligomeric human cyt *c* also bound electrostatically to the LUV more strongly compared to its monomer (Figure 2.7B and Table A.2). In fact, it has been reported that the binding strength of cyt *c* to negatively charged CL is similar among various species of mammalian (*8*).

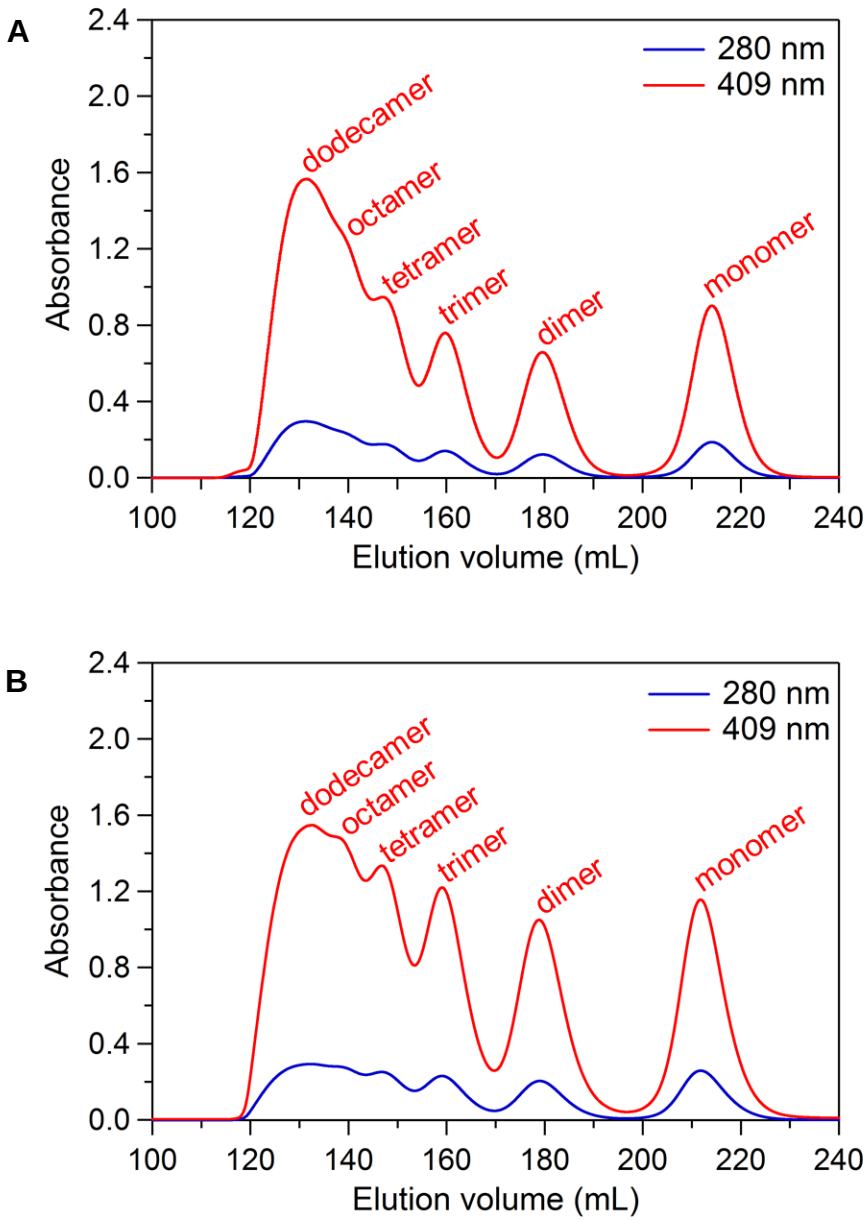

Figure 2.4. Elution curves of monomeric and domain-swapped oligomeric (A) horse and (B) human cyt *c* solution. The elution curve was obtained by gel chromatography (Superdex 75) using the FPLC system. Conditions: flow rate, 1 mL/min; monitoring wavelength, 280 nm and 409 nm; buffer, 50 mM potassium phosphate buffer, pH 7.0; temperature, 4ºC.

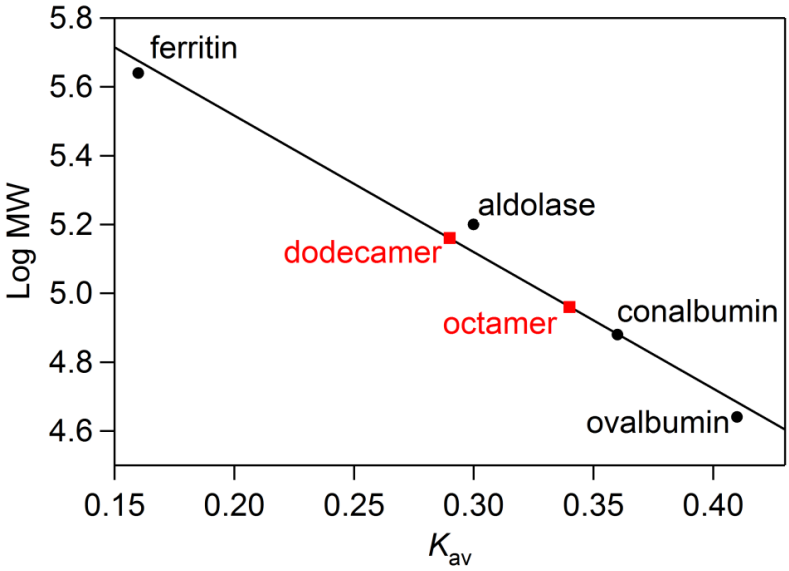

Figure 2.5. Calibration curve for standard proteins on the Superdex 200 column. The standard proteins used were ovalbumin (44 kDa), conalbumin (75 kDa), aldolase (158 kDa), and ferritin (440 kDa). The average molecular weight of octameric and dodecameric horse cyt *c* was determined by interpolating its K_{av} on the calibration curve.

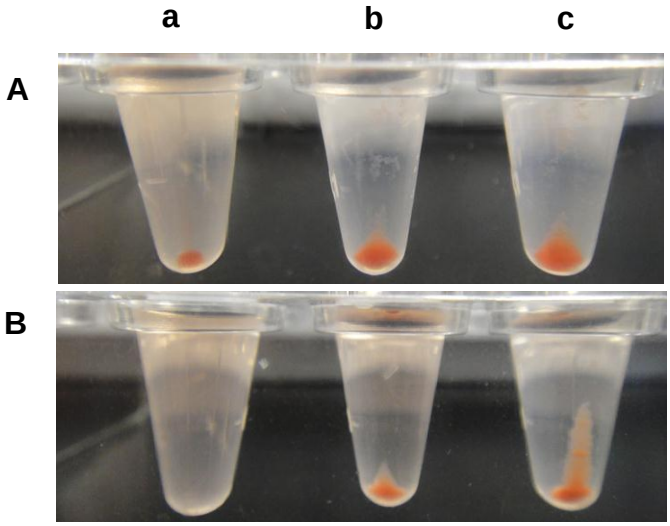

Figure 2.6. Pictures of (a) monomeric, (b) domain-swapped dimeric, and (c) domain-swapped dodecameric ferric horse cyt *c* in the presence of DPPG/DMPC (1:1) LUVs with (A) 10 or (B) 150 mM NaCl. After incubation of cyt *c* with the LUV dispersion at 20ºC for 1.5 h, the mixture was centrifuged at 5,000 g at 20ºC for 5 min. Conditions: lipid, 1 mM; cyt *c*, 25 μM (heme); NaCl, 10 or 150 mM; buffer, 25 mM HEPES-NaOH buffer, pH 7.4.

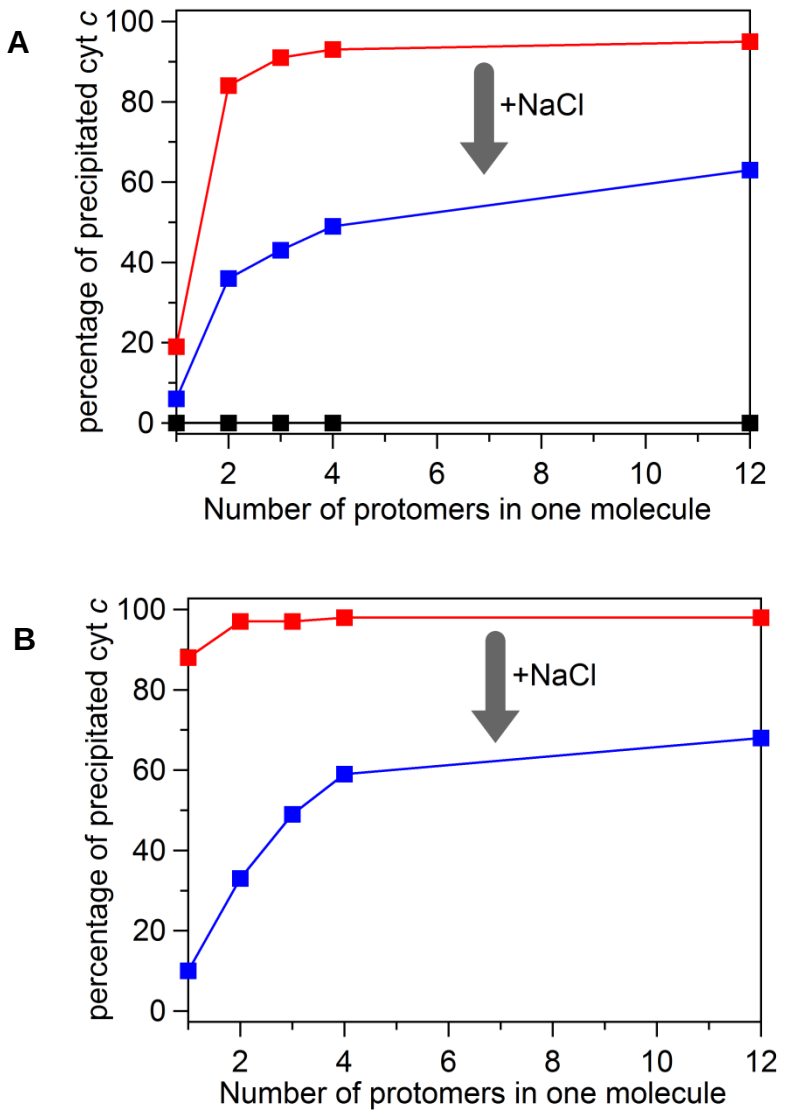

Figure 2.7. Percentage of cyt *c* precipitated by incubation of monomeric and domain-swapped oligomeric ferric (A) horse or (B) human cyt *c* at 20ºC for 1.5 h with DPPG/DMPC (1:1) LUVs in the presence of 10 (red) or 150 mM NaCl (blue) and with DMPC LUVs in the presence of 10 mM NaCl (black). The percentage was calculated from the amount of cyt *c* in the solution after incubation compared to that before incubation. Conditions: lipid, 1 mM; cyt *c*, 25 μM (heme); NaCl, 10 or 150 mM; buffer, 25 mM HEPES-NaOH buffer, pH 7.4.

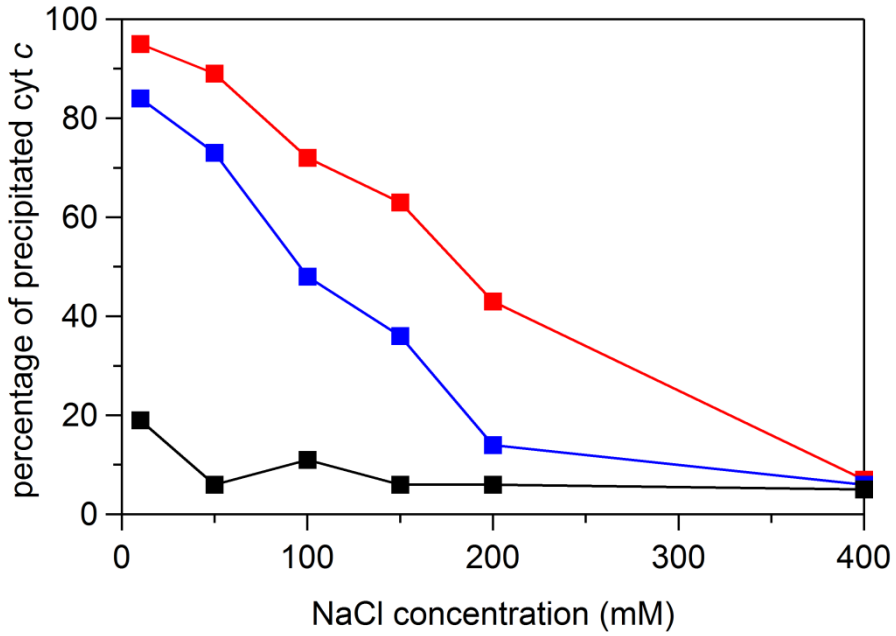

Figure 2.8. Percentage of cyt *c* precipitated by incubation of monomeric (black), domain-swapped dimeric (blue), or domain-swapped dodecameric (red) ferric horse cyt *c* with DPPG/DMPC (1:1) LUVs in the presence of 10, 50, 100, 150, 200, or 400 mM NaCl at 20ºC for 1.5 h. The percentage was calculated from the amount of cyt *c* in the solution after incubation compared to that before incubation. Conditions: lipid, 1 mM; cyt *c*, 25 μM (heme); buffer, 25 mM HEPES-NaOH buffer, pH 7.4.

The amount of dodecameric cyt *c* precipitated by incubation with DPPG/DMPC (1:1) LUVs in the presence of 10 mM NaCl was 95%, whereas those of monomeric, dimeric, trimeric, and tetrameric cyt *c* were 19, 84, 91, and 93%, respectively (Figure 2.7A and Table A.1). These results show that higher order oligomeric cyt *c* interacts more strongly with lipid membranes compared to the monomer and smaller oligomers. It has been reported that the binding constant of positively charged poly(L-lysine) to a negatively charged membrane increases with an increase in the polypeptide chain length

(*26*). Therefore, the enhancement in the lipid membrane binding affinity of domain-swapped oligomeric cyt *c* is attributed to the increase in the positively charged lysine residues in its larger surface area compared to the monomer. Interestingly, the difference between monomeric and dimeric cyt *c* in the amount of protein precipitated by the incubation was relatively large (65% and 30% in the presence of 10 and 150 mM NaCl, respectively), whereas that between dimeric and trimeric cyt *c* was relatively small (7% in the presence of both 10 and 150 mM NaCl) (Figure 2.7A). It has been reported that the binding of cyt *c* to lipid membranes is induced not only by electrostatic interactions but also by hydrophobic interactions (*7, 8, 12, 27*). Since the hydrophobic site of cyt *c* becomes more accessible to the solvent in domain-swapped oligomer compared to the monomer (*24*), the hydrophobic interaction with the membrane may increase in dimeric or highly oligomerized cyt *c*. For further analyses, the effects of domain-swapped dimeric and dodecameric cyt *c* on the membrane were investigated. Domain-swapped dimeric and dodecameric cyt *c* were chosen among other cyt *c* oligomers in order to distinguish the effects of the domain swapping feature and the high positively charged content in the surface.

In the liposome, which is composed of a mixture of anionic and zwitterionic lipids, positively charged proteins and polycationic compounds bind to the anionic

lipids and induce lateral phase separation of the membrane (*28, 29*). Such a lateral phase separation may damage the membrane surface by creating defects at the boundary of different lipid domains (*29, 30*). To investigate the effect of domain-swapped oligomeric ferric horse cyt *c* on the phase separation of DPPG/DMPC (1:1) LUVs, differential scanning calorimetry (DSC) measurements was performed (Figure 2.9). The thermogram of DPPG/DMPC (1:1) LUVs without cyt *c* in HEPES-NaOH buffer, pH 7.4, containing 10 mM NaCl showed an endothermic peak with a phase transition temperature (T_m) at 32.7˚C. This peak corresponds to the transition from the gel to liquid crystalline phase (*31*). DPPG and DMPC in the LUV membrane were homogeneously mixed, since a single peak was observed at 32.7˚C between the T_ms of the pure lipids (24.4˚C and 40.4˚C for DMPC and DPPG, respectively) (Figure 2.9A). For the DSC thermogram of DPPG/DMPC (1:1) LUVs with dodecameric cyt *c* under the same conditions, two T_m peaks were observed at 32.4˚C and 35.0˚C (Figure 2.9D), indicating the presence of two domains in the LUV with different lipid compositions. The DSC thermogram of DPPG/DMPC (1:1) LUVs with dimeric cyt *c* also exhibited two peaks with similar T_m as those detected in the presence of dodecameric cyt *c* (Figure 2.9C). However, there was no change in the T_m of DPPG/DMPC (1:1) LUVs in the presence of monomeric cyt *c* (Figure 2.9B). These results show that oligomeric cyt *c*

induces a lateral phase separation of lipids by interacting with the negatively charged DPPG in the membrane.

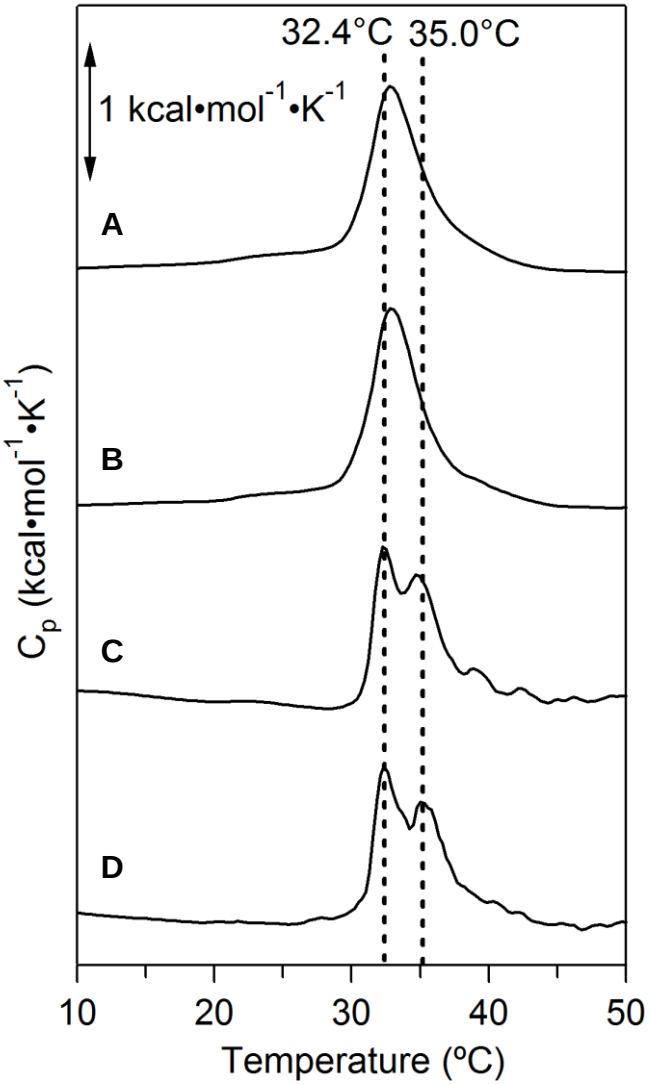

Figure 2.9. DSC thermograms of DPPG/DMPC (1:1) LUVs (A) in the absence of cyt *c* and in the presence of (B) monomeric, (C) domain-swapped dimeric or (D) domain-swapped dodecameric ferric horse cyt *c*. Conditions: lipid, 1 mM; cyt *c*, 25 μM (heme); NaCl, 10 mM; buffer, 25 mM HEPES-NaOH buffer, pH 7.4.

Cell-sized (≥ 1 μm in diameter) giant unilamellar vesicles (GUVs) composed of DPPG/DMPC (1:1) with 1 mol% *N*-(lissamine rhodamine B)-1,2-dihexadecanoyl-*sn*-glycero-3-phosphoethanolamine, triethylammonium salt (*N*-Rh-PE) were monitored to visualize the morphological change of the lipid membrane by interaction with domain-swapped oligomeric cyt *c*. A homogeneous fluorescence of *N*-Rh-PE in the lipid bilayer was observed for the DPPG/DMPC (1:1) GUV in the absence of horse cyt *c*, reflecting a homogeneous mixture of the DPPG and DMPC lipids (Figure 2.10). Dark domains appeared in the GUV at 1 min after an addition of domain-swapped dodecameric ferric horse cyt *c* near the GUV, and the number of the dark domains increased with time (Figure 2.10A). The binding of dodecameric horse cyt *c* to the membrane induced clustering of the DPPG molecules and formation of tightly packed domains, resulting in the exclusion of *N*-Rh-PE from the DPPG-rich domains. Shrinkage of the GUV was observed at 6 min after the addition of dodecameric cyt *c*, and the GUV eventually disrupted. A dark DPPG-rich domain was also observed in the GUV after an addition of domain-swapped dimeric cyt *c* near the GUV, but only at 12 min after the addition (Figure 2.10B). In contrast to dodecameric cyt *c*, the shrinkage of the vesicle by the addition of dimeric cyt *c* was not observed. By an addition of monomeric cyt *c* to the GUV solution, the GUV maintained

a spherical structure without a significant morphological change even at 12 min after the addition (Figure 2.10C). The results show that the binding of dimeric and dodecameric cyt *c* to the negatively charged GUV induces lateral phase separation of lipids, which is consistent with results obtained from the DSC measurements (Figure 2.9). It is noteworthy that dodecameric cyt *c* caused membrane disruption in the GUV, whereas dimeric cyt *c* induced the lateral phase separation without causing significant membrane disruption. These results show that the interaction of cyt *c* with the membrane also depends on the oligomerization degree of domain-swapped oligomeric cyt *c*. In previous studies, formation of anionic phospholipid-enriched domains and morphological change of anionic phospholipid-containing GUV were observed after an addition of monomeric cyt *c* with concentration of 10 μM and 17 μM, respectively (*21*, *22*). By comparing the result in this study and previous studies, monomeric cyt *c* is suggested to induce lipid reorganization and morphological change of membrane only at high protein concentration.

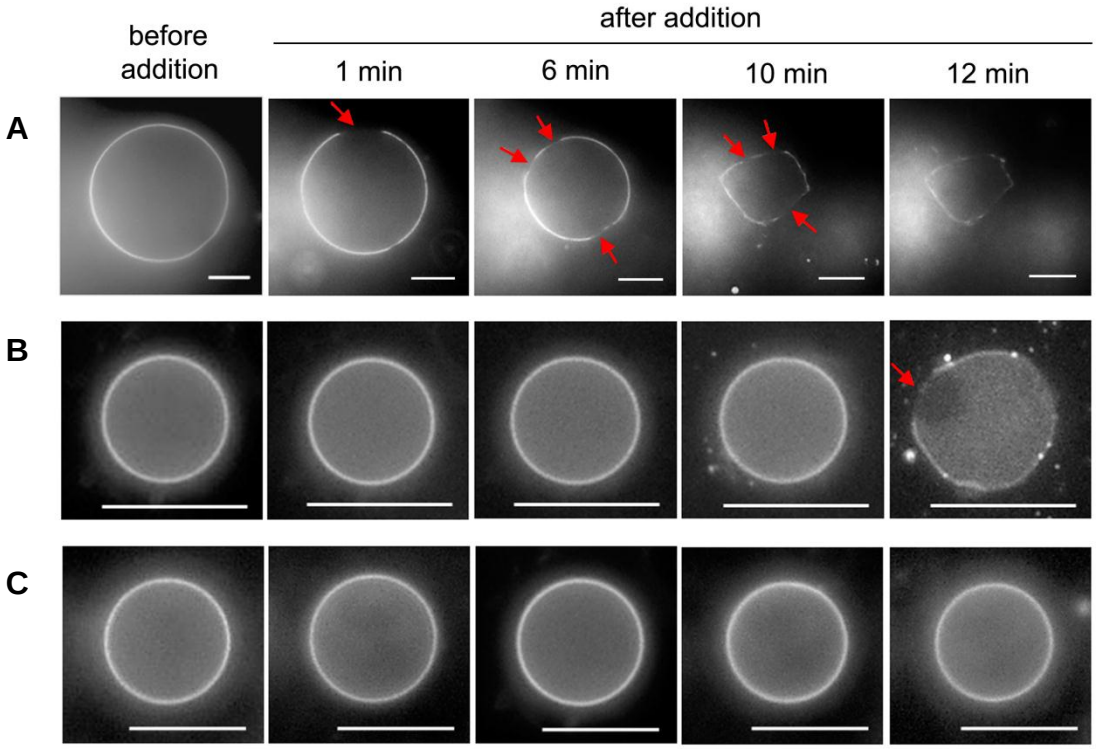

Figure 2.10. Morphological change of GUV induced by an addition of (A) domain-swapped dodecameric, (B) domain-swapped dimeric, or (C) monomeric ferric horse cyt *c* (0.5 μM heme). GUV was composed of DPPG/DMPC (1:1) and labelled with *N*-Rh-PE (1 mol% of lipids). Fluorescence of *N*-Rh-PE was monitored. The red arrows indicate DPPG-rich domains. White bars represent 5 μm.

2-4 Conclusion

Domain-swapped oligomeric horse and human cyt *c* bound electrostatically to the anionic DPPG in DPPG/DMPC vesicles more strongly compared to their monomers. The binding of dodecameric and dimeric horse cyt *c* to the anionic DPPG induced a lateral phase separation of lipids in DPPG/DMPC LUV and GUV, although the binding of the monomer did not. Only dodecameric horse cyt *c* led to membrane disruption in DPPG/DMPC GUV. These results show that cyt *c* can disrupt the membrane of vesicles by forming domain-swapped oligomers.

2-5 References

1. Pettigrew, G. W. (1974) The purification and amino acid sequence of cytochrome *c*-552 from Euglena gracilis, *Biochem. J. 139*, 449-459.

2. Kar, L., Sherman, S. A., and Johnson, M. E. (1994) Comparison of protein structures in solution using local conformations derived from NMR data: application to cytochrome *c*, *J. Biomol. Struct. Dyn. 12*, 527-558.

3. Liu, X., Kim, C. N., Yang, J., Jemmerson, R., and Wang, X. (1996) Induction of apoptotic program in cell-free extracts: requirement for dATP and cytochrome *c*, *Cell 86*, 147-157.

4. Dickerson, R. E., Takano, T., Eisenberg, D., Kallai, O. B., Samson, L., Cooper, A., and Margoliash, E. (1971) Ferricytochrome *c*. I. General features of the horse and bonito proteins at 2.8 A resolution, *J. Biol. Chem. 246*, 1511-1535.

5. Bushnell, G. W., Louie, G. V., and Brayer, G. D. (1990) High-resolution three-dimensional structure of horse heart cytochrome *c*, *J. Mol. Biol. 214*, 585-595.

6. Rytomaa, M., and Kinnunen, P. K. (1994) Evidence for two distinct acidic phospholipid-binding sites in cytochrome *c*, *J. Biol. Chem. 269*, 1770-1774.

7. Rytomaa, M., and Kinnunen, P. K. (1995) Reversibility of the binding of

cytochrome *c* to liposomes. Implications for lipid-protein interactions, *J. Biol. Chem. 270*, 3197-3202.

8. Kalanxhi, E., and Wallace, C. J. (2007) Cytochrome *c* impaled: investigation of the extended lipid anchorage of a soluble protein to mitochondrial membrane models, *Biochem. J. 407*, 179-187.

9. Sinibaldi, F., Howes, B. D., Piro, M. C., Polticelli, F., Bombelli, C., Ferri, T., Coletta, M., Smulevich, G., and Santucci, R. (2010) Extended cardiolipin anchorage to cytochrome *c*: a model for protein-mitochondrial membrane binding, *J. Biol. Inorg. Chem. 15*, 689-700.

10. Kostrzewa, A., Pali, T., Froncisz, W., and Marsh, D. (2000) Membrane location of spin-labeled cytochrome *c* determined by paramagnetic relaxation agents, *Biochemistry 39*, 6066-6074.

11. Sinibaldi, F., Howes, B. D., Droghetti, E., Polticelli, F., Piro, M. C., Di Pierro, D., Fiorucci, L., Coletta, M., Smulevich, G., and Santucci, R. (2013) Role of lysines in cytochrome *c*-cardiolipin interaction, *Biochemistry 52*, 4578-4588.

12. Hanske, J., Toffey, J. R., Morenz, A. M., Bonilla, A. J., Schiavoni, K. H., and Pletneva, E. V. (2012) Conformational properties of cardiolipin-bound cytochrome *c*, *Proc. Natl. Acad. Sci. U. S. A. 109*, 125-130.

13. Heimburg, T., and Marsh, D. (1993) Investigation of secondary and tertiary structural changes of cytochrome *c* in complexes with anionic lipids using amide hydrogen exchange measurements: an FTIR study, *Biophys. J. 65*, 2408-2417.

14. Belikova, N. A., Vladimirov, Y. A., Osipov, A. N., Kapralov, A. A., Tyurin, V. A., Potapovich, M. V., Basova, L. V., Peterson, J., Kurnikov, I. V., and Kagan, V. E. (2006) Peroxidase activity and structural transitions of cytochrome *c* bound to cardiolipin-containing membranes, *Biochemistry 45*, 4998-5009.

15. Sinibaldi, F., Fiorucci, L., Patriarca, A., Lauceri, R., Ferri, T., Coletta, M., and Santucci, R. (2008) Insights into cytochrome *c*-cardiolipin interaction. Role played by ionic strength, *Biochemistry 47*, 6928-6935.

16. Kagan, V. E., Tyurin, V. A., Jiang, J., Tyurina, Y. Y., Ritov, V. B., Amoscato, A. A., Osipov, A. N., Belikova, N. A., Kapralov, A. A., Kini, V., Vlasova, II, Zhao, Q., Zou, M., Di, P., Svistunenko, D. A., Kurnikov, I. V., and Borisenko, G. G. (2005) Cytochrome *c* acts as a cardiolipin oxygenase required for release of proapoptotic factors, *Nat. Chem. Biol. 1*, 223-232.

17. Diederix, R. E. M., Busson, S., Ubbink, M., and Canters, G. W. (2004) Increase of the peroxidase activity of cytochrome *c*-550 by the interaction with detergents, *J. Mol. Catal. B: Enzym. 27*, 75-82.

18. Wang, Z., Matsuo, T., Nagao, S., and Hirota, S. (2011) Peroxidase activity enhancement of horse cytochrome *c* by dimerization, *Org. Biomol. Chem. 9*, 4766-4769.

19. Oellerich, S., Lecomte, S., Paternostre, M., Heimburg, T., and Hildebrandt, P. (2004) Peripheral and integral binding of cytochrome *c* to phospholipids vesicles, *J. Phys. Chem. B 108*, 3871-3878.

20. Brown, L. R., and Wuthrich, K. (1977) NMR and ESR studies of the interactions of cytochrome *c* with mixed cardiolipin-phosphatidylcholine vesicles, *Biochim. Biophys. Acta 468*, 389-410.

21. Haverstick, D. M., and Glaser, M. (1989) Influence of proteins on the reorganization of phospholipid bilayers into large domains, *Biophys. J. 55*, 677-682.

22. Beales, P. A., Bergstrom, C. L., Geerts, N., Groves, J. T., and Vanderlick, T. K. (2011) Single vesicle observations of the cardiolipin-cytochrome *c* interaction: induction of membrane morphology changes, *Langmuir 27*, 6107-6115.

23. Bergstrom, C. L., Beales, P. A., Lv, Y., Vanderlick, T. K., and Groves, J. T. (2013) Cytochrome *c* causes pore formation in cardiolipin-containing membranes, *Proc. Natl. Acad. Sci. U. S. A. 110*, 6269-6274.

24. Hirota, S., Hattori, Y., Nagao, S., Taketa, M., Komori, H., Kamikubo, H., Wang, Z., Takahashi, I., Negi, S., Sugiura, Y., Kataoka, M., and Higuchi, Y. (2010) Cytochrome *c* polymerization by successive domain swapping at the C-terminal helix, *Proc. Natl. Acad. Sci. U. S. A. 107*, 12854-12859.

25. Parui, P. P., Deshpande, M. S., Nagao, S., Kamikubo, H., Komori, H., Higuchi, Y., Kataoka, M., and Hirota, S. (2013) Formation of oligomeric cytochrome *c* during folding by intermolecular hydrophobic interaction between N- and C-terminal alpha-helices, *Biochemistry 52*, 8732-8744.

26. Schwieger, C., and Blume, A. (2007) Interaction of poly(L-lysines) with negatively charged membranes: an FT-IR and DSC study, *Eur. Biophys. J. 36*, 437-450.

27. Tuominen, E. K., Wallace, C. J., and Kinnunen, P. K. (2002) Phospholipid-cytochrome *c* interaction: evidence for the extended lipid anchorage, *J. Biol. Chem. 277*, 8822-8826.

28. Boggs, J. M., Moscarello, M. A., and Papahadjopoulos, D. (1977) Phase separation of acidic and neutral phospholipids induced by human myelin basic protein, *Biochemistry 16*, 5420-5426.

29. Epand, R. M., Rotem, S., Mor, A., Berno, B., and Epand, R. F. (2008) Bacterial

membranes as predictors of antimicrobial potency, *J. Am. Chem. Soc. 130*, 14346-14352.

30. Papahadjopoulos, D., Moscarello, M., Eylar, E. H., and Isac, T. (1975) Effects of proteins on thermotropic phase transitions of phospholipid membranes, *Biochim. Biophys. Acta 401*, 317-335.

31. Wang, P. Y., Lu, J. Z., Chen, J. W., and Hwang, F. (1994) Interaction of the interdigitated DPPG or DPPG/DMPC bilayer with human erythrocyte band 3: differential scanning calorimetry and fluorescence studies, *Chem. Phys. Lipids 69*, 241-249.

Chapter 3

Morphological change of cell membrane

3-1 Introduction

The surface of the plasma membrane of mammalian cells is negatively charged (*1, 2*). The negative charges on the surface of the plasma membrane mainly originate from the sialic acids of glycolipids and glycoproteins, and the chondroitin sulfate and heparan sulfate of proteoglycans (Figure 3.1) (*1-5*). Cyt *c* has been known to neutralize up to 50% of the negative charges on the membrane surface of glomerulus epithelial cells, and the neutralization was reversible in the presence of negatively charged heparin (*6*). The neutralization of the cell charge with cyt *c* was attributed to the electrostatic interaction between the positively charged residues of cyt *c* and the negatively charged molecules on the surface of the plasma membrane.

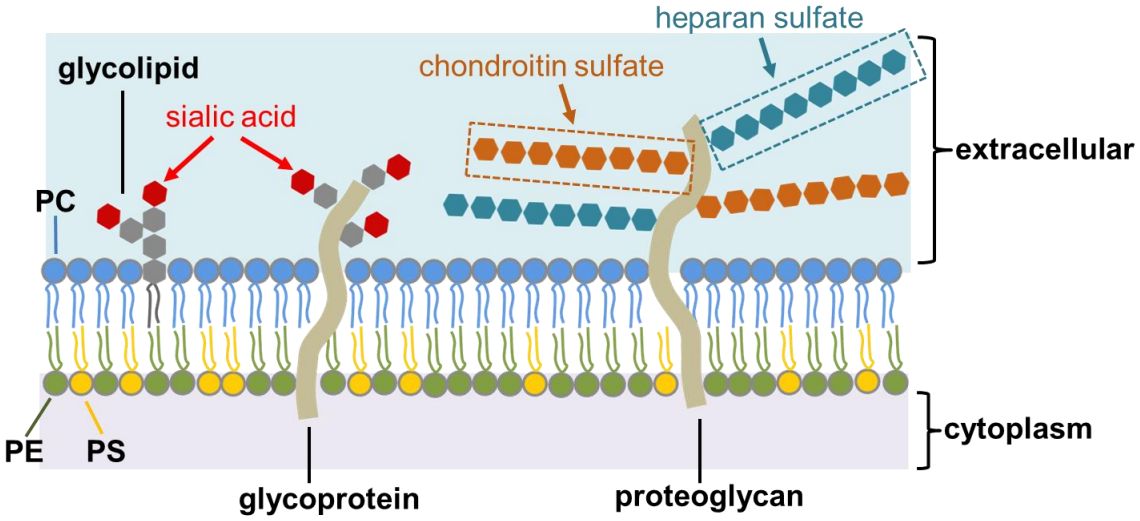

PC : phosphatidylcholine, PE : phosphatidylethanolamine, PS : phosphatidylserine

Figure 3.1. Schematic diagram of the plasma membrane of the mammalian cell.

Domain-swapped oligomeric cyt *c* has been shown to be generated by treatment with alcohol or SDS, where the C-terminal helix is displaced from its original position in the monomer and replaced with the corresponding domain of another cyt *c* molecule (*7*). Domain-swapped oligomeric cyt *c* has a larger surface area and more charges compared to monomeric cyt *c*. The high molecular weight poly($_L$-lysine)s has been shown to bind to the negatively charged cell surface and induced more cytotoxicity than the lower molecular weight poly($_L$-lysine)s (*6, 8-13*). In fact, domain-swapped oligomeric cyt *c* has been shown to interact with a negatively charged liposome and induced lipid phase separation and membrane disruption (Figures 2.6-2.10). To elucidate the effect of domain-swapped oligomeric cyt *c* on an intact cell membrane, the binding of oligomeric cyt *c* to the outer membrane of HeLa cervical cancer cells, and the morphological change of HeLa cells were investigated.

3-2 Materials and methods

3-2-1 Cell culture

HeLa cells (human cervical adenocarcinoma) were obtained from RIKEN Cell Bank (Tsukuba, Japan). The cells were cultured in a humidified atmosphere of 5% CO_2 at 37ºC in Dulbecco's modified Eagle's medium (DMEM) (Nacalai Tesque, Kyoto, Japan) supplemented with 10% (w/v) fetal bovine serum (FBS, Gibco, Grand Island, NY, USA), 100 U/mL penicillin (Gibco), and 100 μg/mL streptomycin (Gibco).

3-2-2 Plasma membrane binding assay

HeLa cells were cultured on a 35-mm dish at a density of 400,000 cells/dish. The density of the cells was counted with a microscope counting chamber (hemocytometer, Erma, Tokyo, Japan). After 24 h of incubation, the cells were washed twice with phosphate-buffered saline (PBS; 137 mM NaCl, 2.7 mM KCl, 10 mM Na_2HPO_4, 1.8 mM KH_2PO_4, pH 7.4) and treated with monomeric, dimeric, trimeric, tetrameric, octameric, and dodecameric ferric cyt *c* (7 μM heme) from horse and human in serum-free medium at 37ºC for 1 h. The medium was discarded, and the cells were subsequently washed twice with PBS buffer. To remove the cyt *c* bound to the plasma membrane, cells were treated with 0.25% (w/v) trypsin (Gibco, Grand Island, NY, USA)

at 37ºC for 3 min. After trypsin was inactivated with 10% (w/v) FBS in DMEM, the cells were washed with PBS buffer and collected by centrifugation at 100 g for 5 min at 20ºC. The cells were disrupted in lysis buffer (20 mM Tris-HCl buffer (pH 7.5), 150 mM NaCl, 1 mM Na_2EDTA, 1 mM EGTA, 1% NP-40, 1% sodium deoxycholate, 2.5 mM sodium pyrophosphate, 1 mM β-glycerophosphate, 1 mM Na_3VO_4, and 1 μg/ml leupeptin; Cell Signalling, Danvers, MA, USA) containing 1 mM phenylmethylsulfonyl fluoride (Wako). The cell extract was passed through a 25-gauge needle 30 times to break the chromosome, and subsequently centrifuged at 17,800 g for 10 min at 4ºC to separate the cell lysate and debris. The total concentration of the proteins in the cell lysate was determined by Bradford assay. An equal amount of protein in every cell lysate was mixed with 2% SDS loading buffer, and applied to 15% polyacrylamide gel for analysis with SDS-polyacrylamide gel electrophoresis (SDS-PAGE). The gel was stained with 3,3',5,5'-tetramethylbenzidine (TMBZ) (TCI, Tokyo, Japan) and hydrogen peroxide for detection of cyt *c*, followed by removal of TMBZ (*14*).

3-2-3 Observation of cell morphology

HeLa cells were cultured on a 15-mm dish at a density of 50,000 cells/dish. The density of the cells was counted with a microscope counting chamber (hemocytometer,

Erma). After 24 h of incubation in DMEM containing 10% FBS, the cells were washed twice with PBS buffer and incubated with monomeric, domain-swapped dimeric, and dodecameric ferric cyt *c* (7 μM heme) from horse and human in serum-free medium at 37ºC for 1 h. The medium was discarded subsequently, and the cells were washed twice with PBS buffer and incubated in DMEM containing 5% FBS for 1 h, 2 h, and 4 h. The cell morphology was observed with a Leica DMI6000 B microscope (Leica, Mannheim, Germany).

3-3 Results and discussion

The binding ability of domain-swapped oligomeric cyt *c* to the outer membrane of HeLa cells was investigated by SDS-PAGE. HeLa cells were incubated with monomeric or oligomeric ferric horse cyt *c*, washed with PBS buffer (137 mM NaCl, 2.7 mM KCl, 10 mM Na_2HPO_4, 1.8 mM KH_2PO_4, pH 7.4) and lysed. Cyt *c* was monitored by staining the SDS-PAGE gel with the peroxidase reaction of the heme using 3,3',5,5'-tetramethylbenzidine (TMBZ) as a substrate (Figure 3.2). In the SDS-PAGE analysis, oligomeric cyt *c* dissociated to monomers by SDS, and was detected as monomers in the gel. A cyt *c* band was observed in the TMBZ-stained gel of the SDS-PAGE when the cells were incubated with dodecameric cyt *c*, whereas no band was observed when incubated with monomeric cyt *c* (Figure 3.2A). The cells were treated with a nonpenetrating enzyme, trypsin, after incubation with cyt *c* to investigate the binding of cyt *c* to the cell surface, since cyt *c* attached to the cell surface may be degraded with trypsin (*15, 16*). The intensity of the cyt *c* band in the SDS-PAGE gel for the cells treated with dodecameric cyt *c* decreased significantly when the cells were treated with trypsin before the analysis. The intensity of the band in the gel also decreased significantly when the cells were incubated with purified oligomeric cyt *c* and treated with trypsin (Figures 3.3B and 3.4B). These results show that oligomeric cyt *c*

was mostly bound to the surface of the outer membrane of the HeLa cell without penetration. The cell lysate from the cells treated with monomeric and dodecameric human cyt *c* exhibited similar properties as those of horse cyt *c* (Figure 3.2B).

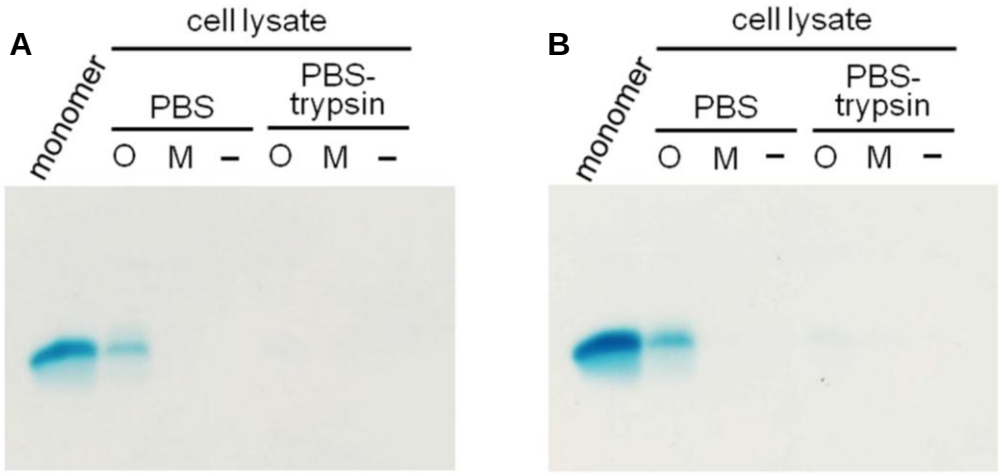

Figure 3.2. SDS-PAGE analysis of cell lysate of HeLa cells. Cell lysates were analyzed after incubation with monomeric (M) or domain-swapped dodecameric (O) horse (A) or human (B) ferric cyt *c* (7 μM heme) and without (−) cyt *c* at 37ºC for 1 h followed by washing with PBS buffer with (PBS) and subsequent treatment with 0.25% (w/v) trypsin (PBS-trypsin). The gel was stained with TMBZ. Monomeric horse or human cyt *c* was used to identify its position in the gel.

Lysates of the HeLa cells were obtained after treatment of the cells with monomeric ferric horse cyt *c* and its domain-swapped dimer, trimer, or tetramer. Monomeric cyt *c* bands were observed for the cell lysates in the SDS-PAGE gel, where the band intensities observed for the cell lysates after treatment with octameric or dodecameric horse cyt *c* were higher than those treated with the monomer or small

oligomers (Figure 3.3A). These results show that the interactions of octameric and dodecameric cyt *c* with the HeLa cell are stronger than those of dimeric, trimeric, and tetrameric horse cyt *c*. Human cyt *c* exhibited a similar behaviour to horse cyt *c*, where the interaction of oligomeric human cyt *c* with the HeLa cells increased in a way that was dependent on the degree of oligomerization (Figure 3.4A). These results demonstrate that oligomeric cyt *c* binds more strongly to HeLa cell membranes compared to the monomer, similar to the case in the model membranes (Figures 2.6 -2.8).

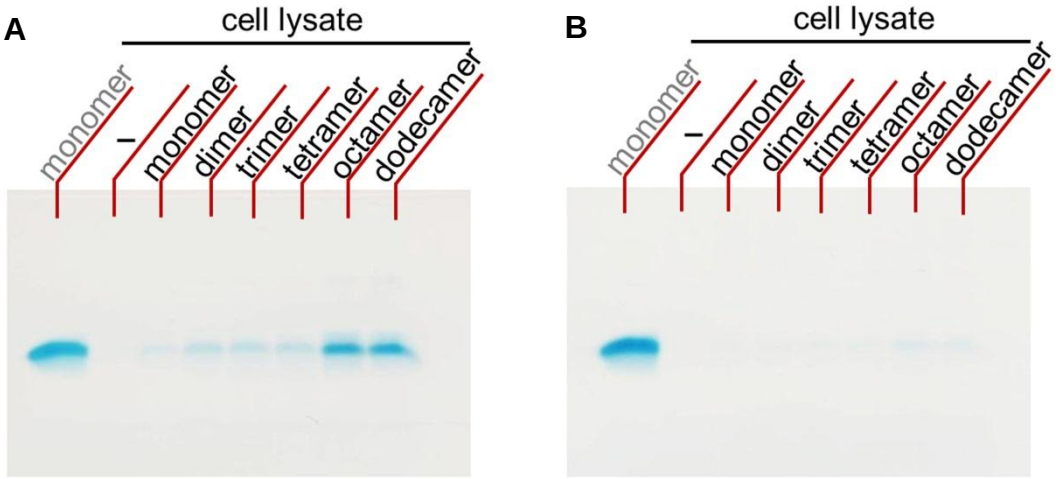

Figure 3.3. SDS-PAGE analysis of cell lysate of HeLa cells obtained after incubation without (—) and with monomeric, domain-swapped dimeric, trimeric, tetrameric, octameric, or dodecameric ferric horse cyt *c* (7 μM heme) at 37ºC for 1 h, followed by washing with (A) PBS buffer and subsequent treatment with (B) 0.25% (w/v) trypsin. The gel was stained with TMBZ. Monomeric horse cyt *c* was used to identify its position in the gel.

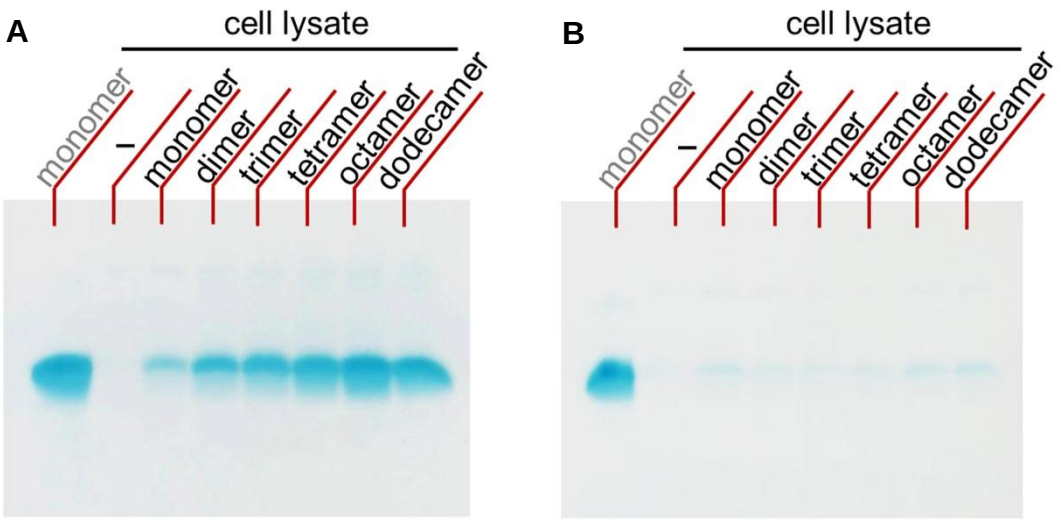

Figure 3.4. SDS-PAGE analysis of cell lysate of HeLa cells obtained after incubation without (—) and with monomeric, domain-swapped dimeric, trimeric, tetrameric, octameric, or dodecameric ferric human cyt *c* (7 μM heme) at 37ºC for 1 h, followed by washing with (A) PBS buffer and subsequent treatment with (B) 0.25% (w/v) trypsin. The gel was stained with TMBZ. Monomeric human cyt *c* was used to identify its position in the gel.

The effect of domain-swapped oligomeric ferric cyt *c* on the morphology of HeLa cells was investigated with a phase contrast microscope. After incubation of the HeLa cells with dodecameric ferric horse cyt *c* for 1 h in the serum free medium, the HeLa cells were washed and incubated in Dulbecco's modified Eagle's medium (DMEM) containing 5% fetal bovine serum (FBS) for 1 h, 2 h, and 4 h. Many cells detached from the culture dish surface and decreased in size after incubation for 2 h and 4 h (Figures. 3.5B and 3.5C). In addition, many protrusions were observed in the cell

surface, showing cell damage. There was no significant different in the number of damaged cells (damaged cells, ~20% counting more than 100 cells) after incubation for 2 h and 4 h. On the other hand, only few damaged cells (damaged cells, ~5%,) were observed after incubation for 1 h (Figure 3.5A).

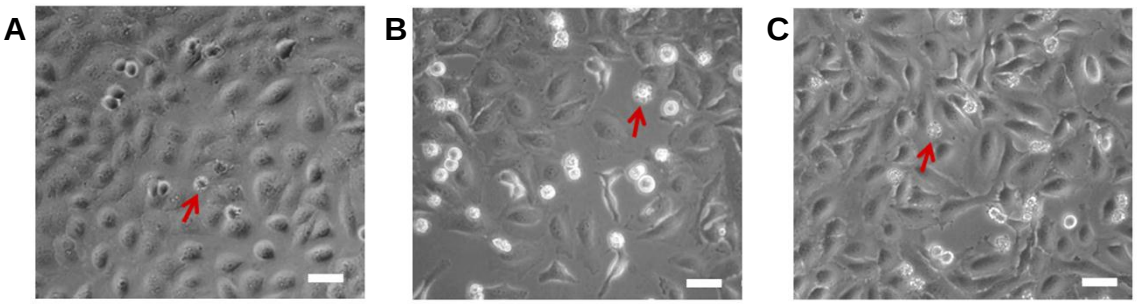

Figure 3.5. Morphological change of HeLa cells after incubation with domain-swapped dodecameric ferric horse cyt *c* for 1 h, followed by washing with PBS buffer and incubation in DMEM containing 5% FBS for (A) 1 h, (B) 2 h, and (C) 4 h. The phase contrast images were obtained with a phase contrast microscope. The red arrows indicate damaged cells. White bars represent 50 μm.

To investigate the effect of monomeric, dimeric, and dodecameric ferric horse cyt *c* on the morphology of HeLa cells, HeLa cells were incubated with monomeric, dimeric, or dodecameric ferric horse cyt *c* for 1 h in the serum free medium, followed by incubation in DMEM containing 5% FBS for 2 h. Similar cell morphological changes were observed by incubation of the cells with dimeric and dodecameric ferric

horse cyt *c* (Figures 3.6A and 3.6B). However, the percentage of cell damage by incubation with dimeric cyt *c* (damaged cells, ~5%, counting more than 100 cells) decreased from that incubated with dodecameric cyt *c* (damaged cells, ~20%) (Figure 3.6B). Little morphological change was observed by incubation of the cells with monomeric cyt *c* or without cyt *c* (Figures 3.6C and 3.6D). Higher order human cyt *c* also caused similar cell morphological changes as higher order horse cyt *c*, where the dodecamer (Figure 3.7A) induced more morphological changes in the cells compared to its monomer (Figure 3.7C) and dimer (Figure 3.7B). These results show that large oligomeric cyt *c* of both human and horse perturbs the biological cells significantly, whereas its monomer and smaller oligomer do not.

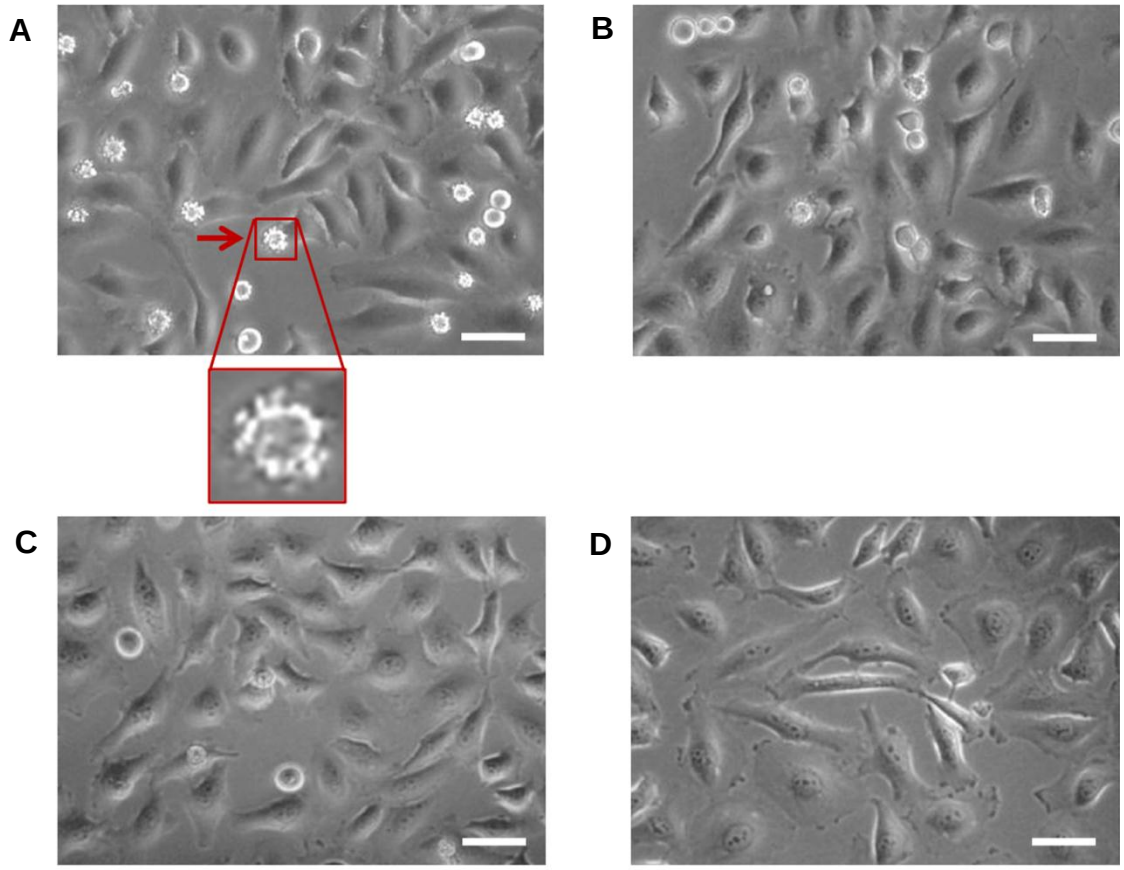

Figure 3.6. Morphological change of HeLa cells after incubation with (A) domain-swapped dodecameric, (B) domain-swapped dimeric, or (C) monomeric ferric horse cyt *c* (7 μM heme) and (D) without horse cyt *c*. The cells were incubated with and without the proteins for 1 h, followed by washing with PBS buffer and incubation in DMEM containing 5% FBS for 2 h. The phase contrast images were obtained with a phase contrast microscope. The red arrow indicates a damaged cell, with an expansion view shown. White bars represent 50 μm.

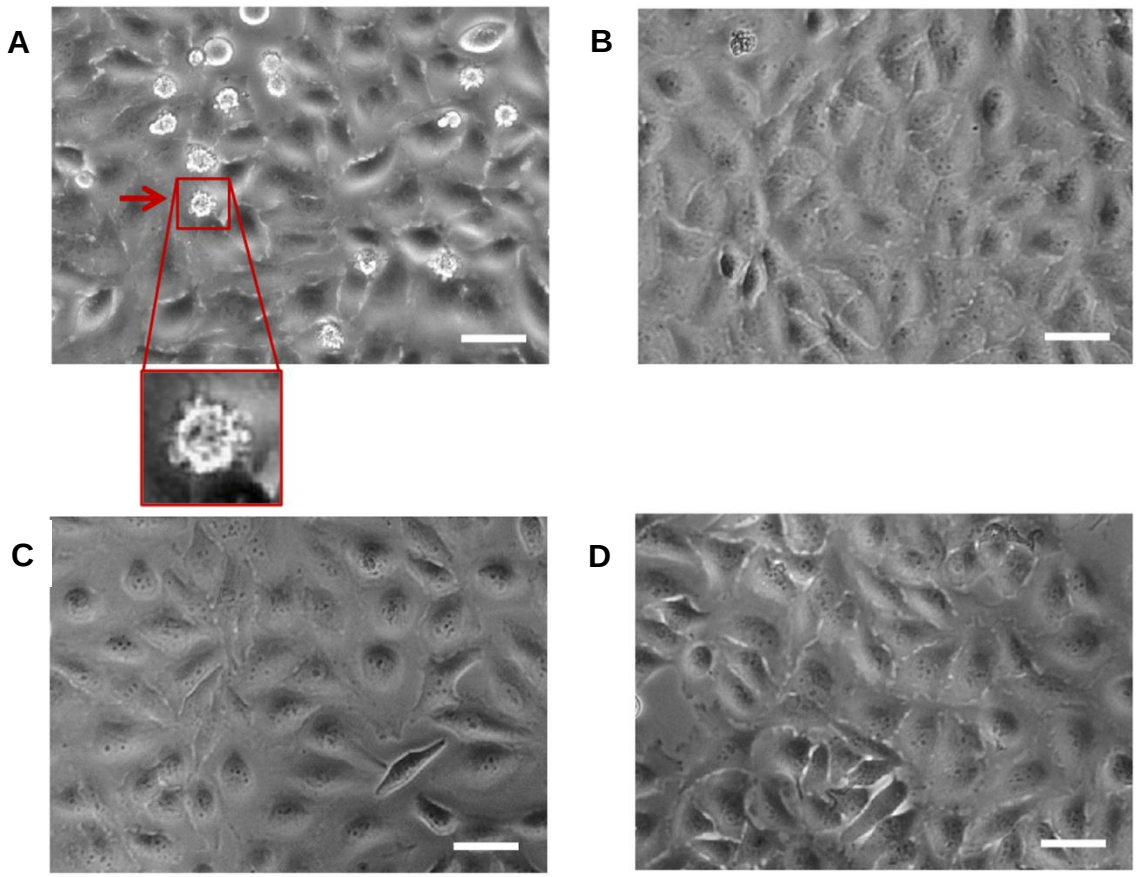

Figure 3.7. Morphological change of HeLa cells after incubation with (A) domain-swapped dodecameric, (B) domain-swapped dimeric, or (C) monomeric ferric human cyt *c* (7 μM heme) and (D) without human cyt *c*. The cells were incubated with and without the proteins for 1 h, followed by washing with PBS buffer and incubation in DMEM containing 5% FBS for 2 h. The phase contrast images were obtained with a phase contrast microscope. The red arrow indicates a damaged cell, with an expansion view shown. White bars represent 50 μm.

Park *et al.* have reported a similar protrusion on the cell surface after an addition of an amphiphilic basic peptide, mastoparan B, to human erythrocytes (*17*). The protrusion of the cell membrane was suggested to be induced by the accumulation of mastoparan B on the surface of the plasma membrane through the electrostatic interaction between positively charged mastoparan B and the negatively charged molecules on the membrane surface. The high coverage of proteins (lateral protein crowding) on a small region (domain) of the membrane can drive positive curvature of the domain, regardless of how the proteins are recruited to the domain (Figure 3.8) (*18-21*). Concentration of the proteins on the domain of the membrane increases lateral steric pressure among the proteins, where the pressure can be reduced by bending the domain, forming the positive curvature. This membrane bending mechanism is called a steric crowding mechanism. A large protein has been showed to bend the domain of the membrane with a smaller overall number of bound proteins per unit area compared to smaller proteins (*20*). The similar phenomenon may be taking place in the binding of domain-swapped oligomeric cyt *c* to HeLa cells. In this study, domain-swapped oligomeric cyt *c* has been showed to bind more strongly to the negatively charged surface membrane of HeLa cells compared to the monomer. The domain-swapped oligomeric cyt *c* may highly cover the negatively charged regions of the cell membrane,

in turn induce the positive curvature of the membrane, which generated protrusions in the cell surface. The formation of protrusions in the cell surface may lead a reduction in the membrane excess area and an increase in surface tension (*22*). The pressure inside the cell would be larger than that outside of the cell. Efflux of water from the inside to outside of the cells may relieve this gradient pressure and reduce the surface tension, leading to a decrease in the cell size. A similar phenomenon may occur for the shrinkage of DPPG/DMPC (1:1) GUV in the presence of domain-swapped dodecameric cyt *c* (Figure 2.10A).

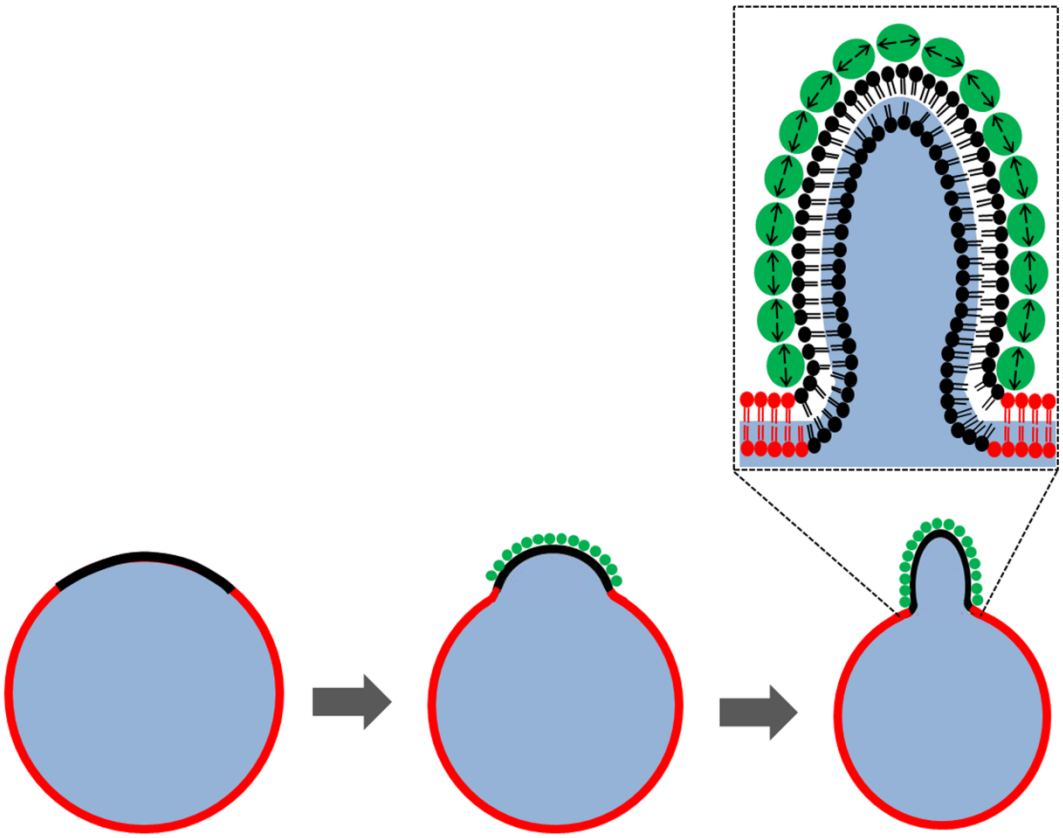

Figure 3.8. Schematic diagram of the steric crowding mechanism. Proteins (green circles) cover the domain (black) of the membrane, where the positive curvature of the domain is induced to reduce the lateral steric pressure among the proteins.

3-4 Conclusion

Domain-swapped oligomeric horse and human cyt *c* bound more strongly to the outer membrane of the HeLa cells compared to their monomers. Dimeric and dodecameric cyt *c* of both horse and human induced damage in the HeLa cells proportional to the membrane binding ability. These results show that cyt *c* can perturb the membranes of biological cells by forming domain-swapped oligomers.

3-5 References

1. Bretscher, M. S., and Raff, M. C. (1975) Mammalian plasma membranes, *Nature 258*, 43-49.

2. Finkelstein, E. I., Chao, P. H., Hung, C. T., and Bulinski, J. C. (2007) Electric field-induced polarization of charged cell surface proteins does not determine the direction of galvanotaxis, *Cell Motil. Cytoskeleton 64*, 833-846.

3. Cook, G. M. (1968) Glycoproteins in membranes, *Biol. Rev. Cambridge Philos. Soc. 43*, 363-391.

4. Kojima, K. (1993) Molecular aspects of the plasma membrane in tumor cells, *Nagoya J. Med. Sci. 56*, 1-18.

5. Traving, C., and Schauer, R. (1998) Structure, function and metabolism of sialic acids, *Cell. Mol. Life Sci. 54*, 1330-1349.

6. Singh, A. K., Kasinath, B. S., and Lewis, E. J. (1992) Interaction of polycations with cell-surface negative charges of epithelial cells, *Biochim. Biophys. Acta 1120*, 337-342.

7. Hirota, S., Hattori, Y., Nagao, S., Taketa, M., Komori, H., Kamikubo, H., Wang, Z., Takahashi, I., Negi, S., Sugiura, Y., Kataoka, M., and Higuchi, Y. (2010) Cytochrome *c* polymerization by successive domain swapping at the C-terminal

helix, *Proc. Natl. Acad. Sci. U. S. A. 107*, 12854-12859.

8. Arnold, L. J., Jr., Dagan, A., Gutheil, J., and Kaplan, N. O. (1979) Antineoplastic activity of poly(L-lysine) with some ascites tumor cells, *Proc. Natl. Acad. Sci. U. S. A. 76*, 3246-3250.

9. Elferink, J. G. (1985) Cytolytic effect of polylysine on rabbit polymorphonuclear leukocytes, *Inflammation 9*, 321-331.

10. Morgan, D. M., Clover, J., and Pearson, J. D. (1988) Effects of synthetic polycations on leucine incorporation, lactate dehydrogenase release, and morphology of human umbilical vein endothelial cells, *J. Cell Sci. 91* 231-238.

11. Morgan, D. M., Larvin, V. L., and Pearson, J. D. (1989) Biochemical characterisation of polycation-induced cytotoxicity to human vascular endothelial cells, *J. Cell Sci. 94* 553-559.

12. Choksakulnimitr, S., Masuda, S., Tokuda, H., Takakura, Y., and Hashida, M. (1995) In vitro cytotoxicity of macromolecules in different cell culture systems, *J. Control. Release 34*, 233-241.

13. Fischer, D., Li, Y., Ahlemeyer, B., Krieglstein, J., and Kissel, T. (2003) In vitro cytotoxicity testing of polycations: influence of polymer structure on cell viability and hemolysis, *Biomaterials 24*, 1121-1131.

14. Thomas, P. E., Ryan, D., and Levin, W. (1976) An improved staining procedure for the detection of the peroxidase activity of cytochrome P-450 on sodium dodecyl sulfate polyacrylamide gels, *Anal. Biochem. 75*, 168-176.

15. Karp, G. (1996) *Cell and molecular biology: concepts and experiments*, John Wiley & Sons, New York.

16. Gump, J. M., June, R. K., and Dowdy, S. F. (2010) Revised role of glycosaminoglycans in TAT protein transduction domain-mediated cellular transduction, *J. Biol. Chem. 285*, 1500-1507.

17. Park, N. G., Kim, C. H., Chung, J. K., Huh, M. D., Park, J. S., and Kang, S. W. (1998) Morphological changes of biomembranes by amphiphilic basic peptides mastoparan B and 4_3, *J. Microbiol. 36*, 179-183.

18. Stachowiak, J. C., Hayden, C. C., and Sasaki, D. Y. (2010) Steric confinement of proteins on lipid membranes can drive curvature and tubulation, *Proc. Natl. Acad. Sci. U. S. A. 107*, 7781-7786.

19. Kirchhausen, T. (2012) Bending membranes, *Nat. Cell Biol. 14*, 906-908.

20. Stachowiak, J. C., Schmid, E. M., Ryan, C. J., Ann, H. S., Sasaki, D. Y., Sherman, M. B., Geissler, P. L., Fletcher, D. A., and Hayden, C. C. (2012) Membrane bending by protein-protein crowding, *Nat. Cell Biol. 14*, 944-949.

21. Stachowiak, J. C., Brodsky, F. M., and Miller, E. A. (2013) A cost-benefit analysis of the physical mechanisms of membrane curvature, *Nat. Cell Biol. 15*, 1019-1027.

22. Li, S., and Malmstadt, N. (2013) Deformation and poration of lipid bilayer membranes by cationic nanoparticles, *Soft Matter 9*, 4969-4976.

Chapter 4

Conclusion

In liposomes and HeLa cells, domain-swapped oligomeric cyt *c* displayed higher binding affinity to the membranes, causing larger morphological changes compared to the monomer (Figures 2.6-2-10 and Figures 3.2-3.7). Domain-swapped oligomeric cyt *c* contains protomers which connected each other by domain swapping. I attribute the higher membrane binding affinity of domain-swapped oligomeric cyt *c* to the increase in the number of positive charges from the lysine residues on the surface of one molecule with a larger surface area compared to the monomer and dimer (Figure 4.1). In domain-swapped oligomeric cyt *c*, the electrostatic interaction of a protomer with the membrane was suggested to be stabilized by the electrostatic interaction of other protomers with the membrane. It has been reported that the hydrophobic cavity of cyt *c* and the acyl chain of CL interacts hydrophobically. The hydrophobic group is more accessible to the solvent in domain-swapped oligomeric cyt *c* compared to the monomer, and the hydrophobic interaction may also contribute to the binding of oligomeric cyt *c* to the lipids. Although dimeric cyt *c* caused phase separation in the DPPG/DMPC (1:1) LUV and GUV (Figures 2.9 and 2.10), the electrostatic and hydrophobic interactions were probably not strong enough to initiate disruption of the cells (Figure 4.1B). For the large oligomers, the protein interacted more strongly with the membrane by the

increased positive charge and hydrophobicity in its surface compared to the monomer and dimer, which caused significant damage to the cells (Figure 4.1C).

Domain-swapped oligomeric horse and human cyt *c* bound more strongly to anionic phospholipid-containing vesicles and to the outer membrane of HeLa cells compared to the monomer. Oligomeric horse cyt *c* also induced a lateral phase separation in DPPG/DMPC LUV and GUV, leading to membrane disruption. Dimeric and dodecameric cyt *c* of both horse and human induced damage in the HeLa cells proportional to the membrane binding ability. These results show that domain-swapped oligomeric proteins may exhibit different properties to cell systems compared to its monomer. For future study, properties of the oligomers may be applied to protein engineering and medical application such as antibacterial drugs.

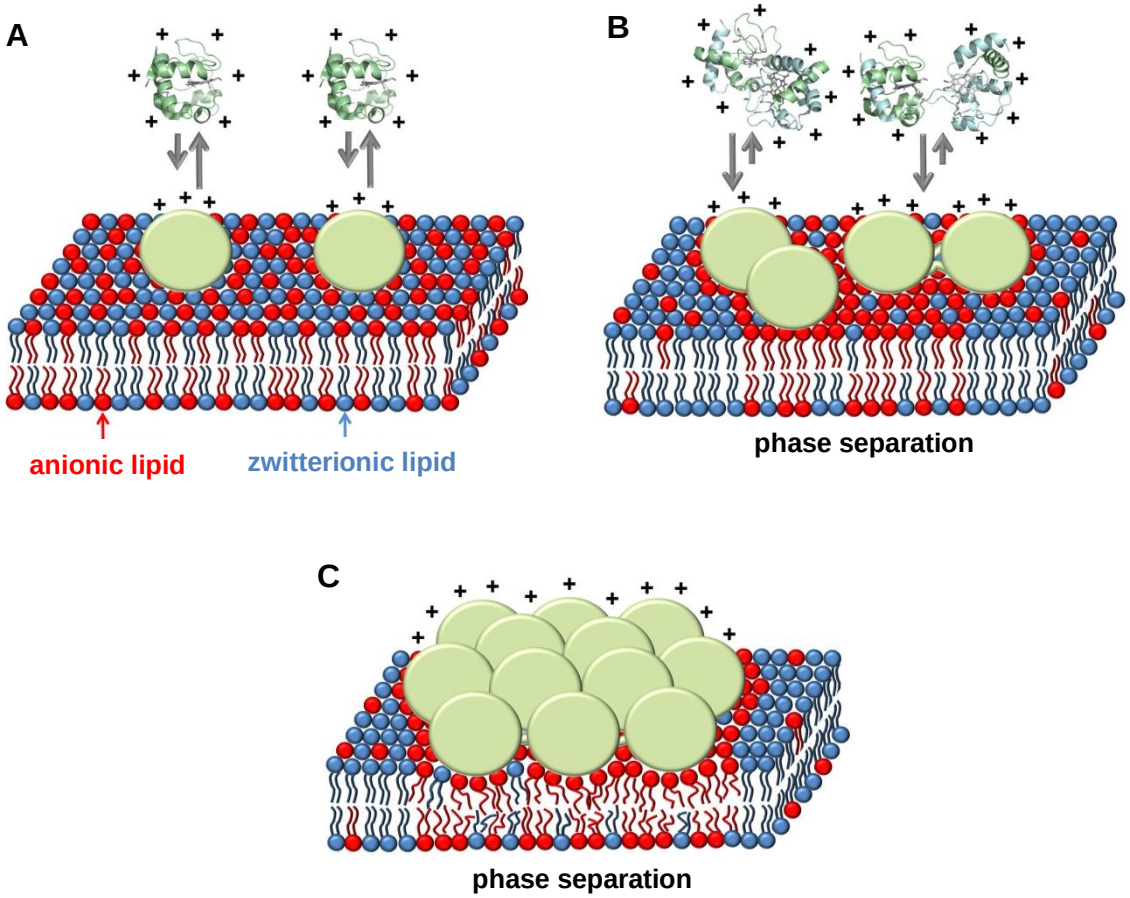

Figure 4.1. Schematic view for interaction of (A) monomeric, (B) domain-swapped dimeric, and (C) domain-swapped higher order cyt *c* with a negatively charge cell membrane. Light green circles on the membrane represent cyt *c* monomer and oligomers.

ACKNOWLEDGMENTS

First of all, I am grateful to the Almighty God for the wisdom and perseverance that He has been bestowed upon me during the doctoral research, and indeed, throughout my life: "I can do everything through Him who give me strength." (Philippians 4: 13). I would like to express my sincere gratitude to my academic supervisor, Professor Shun Hirota, for the continuous support in my doctoral study and research, for his patience, enthusiasm, and immense knowledge. His guidance helped me in all the time of research, and writing of the thesis and paper.

Besides my academic supervisor, I would like to express my gratitude to my supervisor committee, Professor Jun-ichi Kikuchi, Professor Kiyomi Kakiuchi, and Professor Takashi Matsuo, for their insightful comments, and valuable suggestions.

I would like to express the deepest appreciation to Monbukagakusho for the financial support for 3.5 years, and to Professor Marchaban and Professor Edy Meiyanto for giving me a recommendation to apply Monbukagakusho scholarship.

I would like to offer my special thanks to Dr. Satoshi Nagao for his support, guidance, advice throughout the doctoral research, as well as his painstaking effort in proofreading the thesis and paper draft, are greatly appreciated. My sincere thanks also

go to Dr. Kazuma Yasuhara for his expert and sincere guidance in vesicle experiment.

I would like to thank Professor Zhonghua Wang, Dr. Masaru Yamanaka, Dr. Ari Dwi Nugraheni, Dr. Halan Prakash, Dr. Megha Subhash Deshpande, Yugo Hayashi, Akira Fujii, Yuuki Ando, Mariko Ueda, Nobuhiro Yamashiro, Yukie Kitada, Ryuzaki Michiko, Hao Fei, and Manami Tsukamoto for their support in experiment, and for the constructive discussions. I owe a very important debt to Dr. Riris Istighfari Jenie and Dr. Nunung Yuniarti for their advices in mammalian cells experiment. I also take this opportunity to record my sincere thanks to all members of Supramolecular Science Laboratory for their support, friendship and warm encouragement.

Special thanks to Endah Puji Septi Setyani and Dr. Ari Dwi Nugraheni for introducing me to Professor Shun Hirota. My time here would have been immeasurably more difficult without the help of Kaoru Teshima and the staff of NAIST Student Affair Section who deliver the important information and assist the daily life.

My life in Japan has been blessed with a great caring pastor, Ayub Abner Martinus Mbuilima, and brothers and sisters at Osaka Fukuin Kyoukai Indonesia (GIII Osaka) who unceasingly pray and encourage me in walking with God. Last but not least, my heartfelt appreciation goes to my family for their unconditional encouragement, pray, and support throughout my life.

LIST OF PUBLICATION

Publication

Morphological change of cell membrane by interaction with domain-swapped cytochrome *c* oligomers

Sendy Junedi, Kazuma Yasuhara, Satoshi Nagao, Jun-ichi Kikuchi, and Shun Hirota,

ChemBioChem, DOI: 10.1002/cbic.201300728.

Conference

Binding of oligomeric cytochrome *c* to cell membrane

Sendy Junedi, Kazuma Yasuhara, Satoshi Nagao, Jun-ichi Kikuchi, and Shun Hirota

The 51st Annual Meeting of The Biophysical Society of Japan, Kyoto International Conference Center, Kyoto, October 28-30, 2013. (Poster Presentation)

APPENDIX

Table A.1. Percentage of cyt *c* precipitated by incubation of horse cyt *c* with DPPG/DMPC (1:1) LUVs.

Number of protomers	Percentage of precipitated cyt *c* (%)	
	in 10 mM NaCl	in 150 mM NaCl
1	19	6
2	84	36
3	91	43
4	93	49
12	95	63

Conditions: lipid, 1 mM; cyt *c*, 25 μM (heme); buffer, 25 mM HEPES-NaOH buffer, pH 7.4.; incubation temperature, 20ºC; incubation time, 1.5 h.

Table A.2. Percentage of cyt *c* precipitated by incubation of human cyt *c* with DPPG/DMPC (1:1) LUVs.

Number of protomers	Percentage of precipitated cyt *c* (%)	
	in 10 mM NaCl	in 150 mM NaCl
1	88	10
2	97	33
3	97	49
4	98	59
12	98	68

Conditions: lipid, 1 mM; cyt *c*, 25 μM (heme); buffer, 25 mM HEPES-NaOH buffer, pH 7.4.; incubation temperature, 20ºC; incubation time, 1.5 h.

Table A.3. Percentage of cyt *c* precipitated by incubation of monomeric, dimeric, and dodecameric horse cyt *c* with DPPG/DMPC (1:1) LUVs in the presence of different NaCl concentration.

Concentration of NaCl (mM)	Percentage of precipitated cyt *c* (%)		
	monomer	dimer	dodecamer
10	19	84	95
50	6	73	89
100	11	48	72
150	6	36	63
200	6	14	43
400	5	6	7

Conditions: lipid, 1 mM; cyt *c*, 25 μM (heme); buffer, 25 mM HEPES-NaOH buffer, pH 7.4.; incubation temperature, 20ºC; incubation time, 1.5 h.